UNIVERSITÀ DEL PIEMONTE ORIENTALE

SCHOOL OF MEDICINE

Department of Health Sciences

Master's degree in Medical Biotechnologies

Molecular and functional characterization of the cellular deacetylase SIRT1 network in HPV-driven cancer

Mentor: Prof. Marisa Gariglio

Correlator: Prof. Irene Lo Cigno

Candidate: Mattia Pozzi

Matricula number: 20028304

Academic year 2023/2024

INDEX

1. ABSTRACT

Human papillomavirus (HPV)-associated cancers of the genital and head and neck region account for ~5% of all global cancer cases. The pathogenesis of these malignancies is predominantly driven by the dysregulated expression of the viral oncoproteins E6 and E7, which target p53 and pRb proteins, respectively, and promote cellular proliferation abrogating cell cycle checkpoints. The laboratory of Molecular Virology headed by Professor Gariglio has recently uncovered a novel route used by high-risk HPVs to effectively suppress p53 activity centered around the cellular deacetylase SIRT1. Specifically, it was found that inhibition of SIRT1 in HPV+ cell lines reinstated a transcriptionally active K382-acetylated p53, leading to cell cycle arrest and reducing cell survival when compared to HPV- cells. In addition, it was demonstrated that treatment with the SIRT1 inhibitor namely EX527, enhanced the sensitivity of HPV+ cells to sublethal doses of standard genotoxic agents both *in vitro,* including NOKE6/E7 cells*,* and *in vivo* in a syngeneic mouse model obtained by dorsal subcutaneous injection of C3.43 cells, harboring an integrated HPV16 genome, into C57BL/6J mice (Lo Cigno et al., 2023). Consistently, in this thesis we aimed to validate the anticancer efficacy of EX527 in NOKE6/E7 organotypic raft cultures and in xenografts of NOKE6/E7 into NOD SCID γ-null (NSG) mice. In particular, we found that NOKE6/E7 raft cultures treated with EX527 showed a reduced epithelial thickness compared to those treated with vehicle as confirmed by a lower EdU incorporation and a reduction in the percentage of cells positive for the proliferation marker MCM7. Moreover, NOKE6/E7 invasiveness was found significantly decreased. Same results were obtained in the xenograft models where EX527 treatment leads to a reduction of the tumor burden, a decrease of the number of cells positive for the cellular proliferation marker Ki67, and p53 restoration. In addition, mass-spectrometry (MS) analysis of the proteins co-immunoprecipitated with SIRT1 from NOKE6/E7 cellular extracts allowed to isolate the SIRT1 interactome. STRING and GO term analyses identified a network of interacting proteins involved in “DNA repair” and “nuclear DNA replication”, including MCM7 and MCM4, belonging to the mini-chromosome maintenance (MCM) protein family. Therefore, we aimed to validate the SIRT1 interactome by immunoprecipitation and proximity ligation assay (PLA) to demonstrate the existence of a DNA-binding platform consisting of SIRT1 and the MCM complex at the replication origin necessary to prevent excess replication and preserve genomic stability. Altogether, these findings reveal a novel role of SIRT1 during HPV-driven oncogenesis, influencing not only p53 stability but also DNA replication. We propose that hrHPVs hijack SIRT1 to modulate these pathways through deacetylation.

2. INTRODUCTION

2.1 PAPILLOMAVIRUSES

2.1.1 General features and classification

Papillomaviruses (PVs) are small, icosahedral, non-enveloped viruses with a double-stranded DNA of approximately 8 kilobases (kbp) in length. They belong to the *Papillomaviridae* family which consists in over 400 genotypes with a pronounced tropism for stratified squamous epithelia. PVs can induce cutaneous and mucosal hyperplastic lesions in a wide range of vertebrates (Egawa et al., 2015). Papillomavirus types are also classified according to the genome sequence of the L1 open reading frame, the most conserved gene coding for the major capsid protein (Burk et al., 2013). Human papillomaviruses (HPVs) are grouped into five genera, *alpha, beta, gamma, mu,* and *nu.* Different genera show different life cycle and disease association (Doorbar et al., 2015). HPVs are divided into "cutaneous" or "mucosal", depending on the capacity to infect basal epithelial cells of the skin or mucosa. Cutaneous HPVs, mainly found in beta and gamma genera, infect the skin of immunocompromised individuals only, while, mucosal ones, belonging to the alpha genus, affect both cutaneous and mucosal tissues of healthy subjects. Mucosal HPVs are also defined as either "low-risk" or "high-risk" HPVs based on the propensity for malignant progression (Egawa et al., 2015; Nelson & Mirabello, 2023). Low-risk genotypes produce, in most individuals, asymptomatic infections or benign lesions such as common warts, genital warts (condyloma acuminata) and papillomas. However, problematic pathologies (e.g. recurrent respiratory papillomatosis and epidermodysplasia verruciformis), eventually associated with cancer development, can appear in case of immunodepression or genetic predisposition (Egawa & Doorbar, 2017). The most common low-risk HPVs are HPV6 and 11.

High-risk HPVs (hrHPVs), instead, are associated with cervical or other anogenital cancers and with head and neck cancers, particularly oropharyngeal cancer. HPV accounts for ~5% of all cancers worldwide. Papillomavirus infection is the etiological factor of over the 95% and the 70% of cervical and oropharyngeal cancer cases, respectively (Gheit, 2019; Johnson et al., 2020). Twelve hrHPVs (16, 18, 31, 33, 35, 39, 45, 51, 52, 56, 58, 59) are considered carcinogenic for the humans, whereas other genotypes (HPV26, 53, 66, 67, 68, 70, 73, 83) are classified as possible or probably carcinogenic (Gheit, 2019).

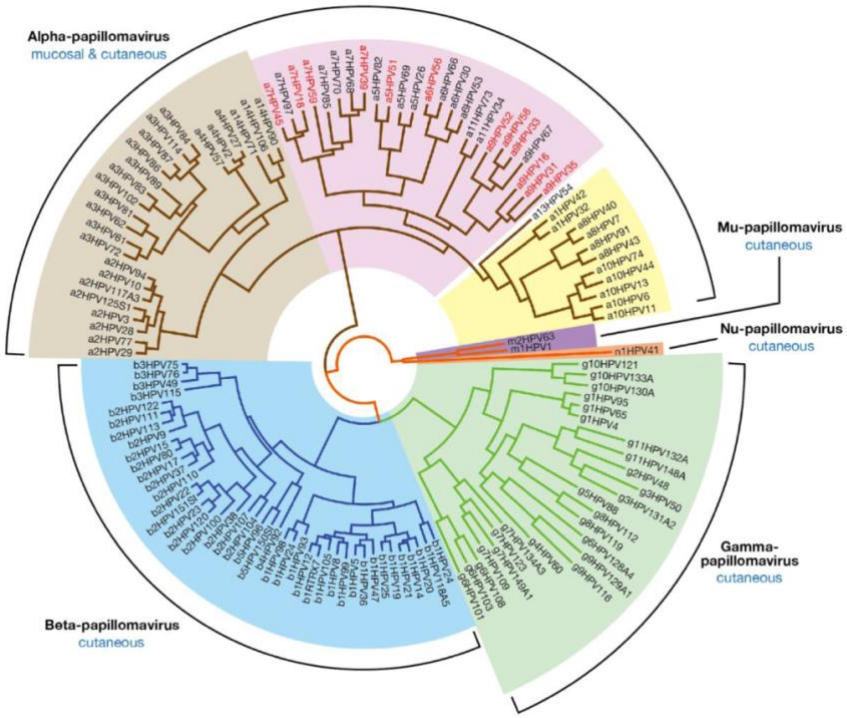

Figure 1. Human papillomavirus types found in humans fall into five genera and alpha, beta (blue) and gamma (green) represent the largest groups. Alpha genus comprises low-risk cutaneous (light brown), low-risk mucosal (yellow) and high-risk (pink) types according to their association with the development of cancer. High-risk types highlighted in red are confirmed as carcinogens for humans based on epidemiological data, while the remaining are probable or possible carcinogens. Beta, gamma, mu, and nu-papillomaviruses are responsible for cutaneous lesions. The evolutionary tree is based on alignment of the E1, E2, L1, and L2 genes (Egawa et al., 2015).

2.1.2 Structure and genome organization

Human papillomaviruses carry a circular double-stranded DNA within an icosahedral capsid of about 55 nm in diameter. Viral organization is strictly maintained in all HPV family members and consists of three functional regions with a total of eight open reading frames (ORFs) coding for both structural and non-structural proteins. Two polyadenylation sites separate the three regions from each other. The upstream regulatory region (URR), or long control region (LCR), contains regulatory elements, including transcription factor-binding sites, enhancer and promoter elements, and the viral origin of DNA replication (ori). The early (E) and the late (L) regions represent the codifying portion of the viral DNA and code for non-structural and structural proteins, respectively (Moody, 2022; Scarth et al., 2021; Yu et al., 2022).

E1 protein is an ATP-dependent hexameric DNA helicase essential for viral replication. It is involved in increasing the copy number of the viral episome upon infection of basal

keratinocytes and in maintaining a constant level of episomes in cells migrating upward the epithelium. In addition, E1 also promotes the amplification of the viral genome during the productive phase of the viral life cycle (Bergvall et al., 2013). Instead, E2 is the main transcriptional regulator of HPV. It primarily recruits cellular factors to the viral genome, activating or repressing transcriptional processes. Mutations of the viral genome or integration into the host genome are the principle causes of occasional loss of E2 functions, which leads to alleviation of E2-mediated repression with an increased expression of the E6 and E7 genes (McBride, 2013).

E4 protein has a role in genome amplification, expression of capsid proteins and virus assembly, transmission, and release. Its abundance in lesions makes the protein a suitable and specific biomarker of active infection and disease severity, especially in case of hrHPV infection (Doorbar, 2013). Additionally, E4 is thought to have a role also in virus escape from cornified epithelial layers (Egawa et al., 2015).

E5, E6 and E7 are the proteins responsible for HPV-dependent malignant transformation. They interact with many host cell proteins deregulating essential cellular functions and, thus, promoting several hallmarks of cancer. E6 and E7 proteins have a key role in cell cycle deregulation, cell immortalization and invasion, and immune system modulation. Furthermore, they interfere with DNA damage repair. In particular, E6 from hrHPVs binds to and promotes degradation of the tumor suppressor protein p53, leading to uncontrolled cell proliferation and apoptosis arrest, whereas hrHPV E7 targets the retinoblastoma tumor suppressor (pRb) protein inducing its ubiquitination and eliciting E2F-mediated transcriptional activation of S-phase genes. Even though less characterized, E5 is thought to sustain proliferative signalling and to modulate the immune system (Estêvão et al., 2019). However, low-risk HPVs lack E5 or encode different types of the protein with less transforming ability (de Freitas et al., 2017). L1 and L2 proteins are the major and the minor capsid proteins, respectively. They both have a role in the process of virion assembly. L1 is also involved in the initial interaction of the capsid with the host through interactions with heparan sulphate carbohydrates displayed on proteoglycans (Buck et al., 2013), whereas L2 is implicated also in the infectious process (J. W. Wang & Roden, 2013).

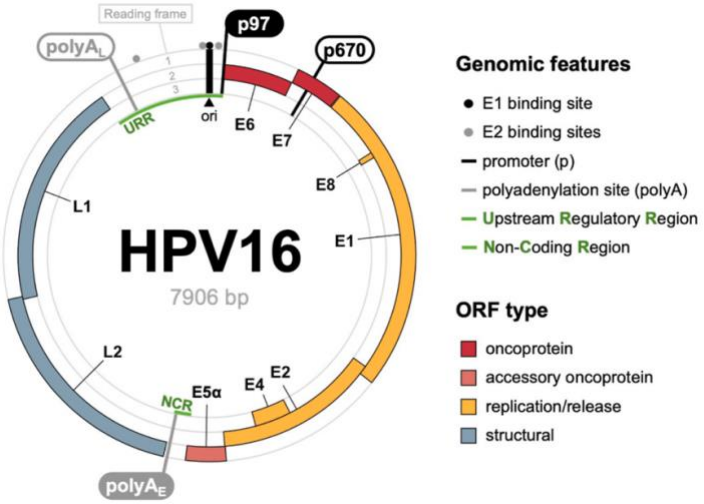

Figure 2. HPV genome has a double-stranded DNA structure. Genes are transcribed in a single direction (clockwise) and encode for non-structural (E1, E2, E4, E5, E6, and E7) and structural (L1, L2) proteins. The upstream regulator region (URR) acts as the regulator of DNA replication and contains the origin of replication (ori). p97 and p670 are the major promoters (Nelson & Mirabello, 2023).

2.1.3 HPV life cycle

HPVs infect keratinocytes of the cutaneous and mucosal stratified epithelia, which are composed of a basal layer with self-renewing cells that divide symmetrically to replenish the layer, and asymmetrically to generate daughter cells that make up the differentiated layers. HPV life cycle is linked to the differentiation program of epithelial keratinocytes (McBride, 2022). Firstly, viral particles have access to the basal layer via microlesions, hair follicles or by entering cells at the squamo-columnar junctions; then viral progeny is produced in differentiated daughter cells in the uppermost epithelial layers; lastly new virions are released from the surface of the epithelium in exfoliating squames or superficial keratinocytes (Harden & Munger, 2017; McBride, 2022). Consequently, HPV life cycle takes ~3 weeks: the time needed for an epithelial cell to differentiate and migrate from the basal to the superficial layer, undergo senescence and die.

To establish an infection, the first interaction between HPV and the host is the viral L1 capsid protein-mediated binding with the heparin sulphate proteoglycans, located on the basement membrane or on the surface of basal layer cells. This binding leads to a cyclophilin B-mediated conformational change in the capsid that allows the exposure of the N-terminus of the L2 protein. Then, the N-terminus is cleaved by furin protease and/or related cellular proprotein convertases (e.g. PC5, 6) enabling the linkage to a still unknown secondary receptor on the membrane of the target cell (Graham, 2017; J. W. Wang & Roden, 2013). Once internalized by

endocytosis, virions travel through the endosomal system, undergo uncoating, and enter the nucleus, coupled with the L2 protein, through a tubulin-dependent pathway. L2 also ensures the correct nuclear entry of the viral episomal genome, while L1 protein is retained in the endosome and ultimately subjected to lysosomal degradation (Doorbar et al., 2012).

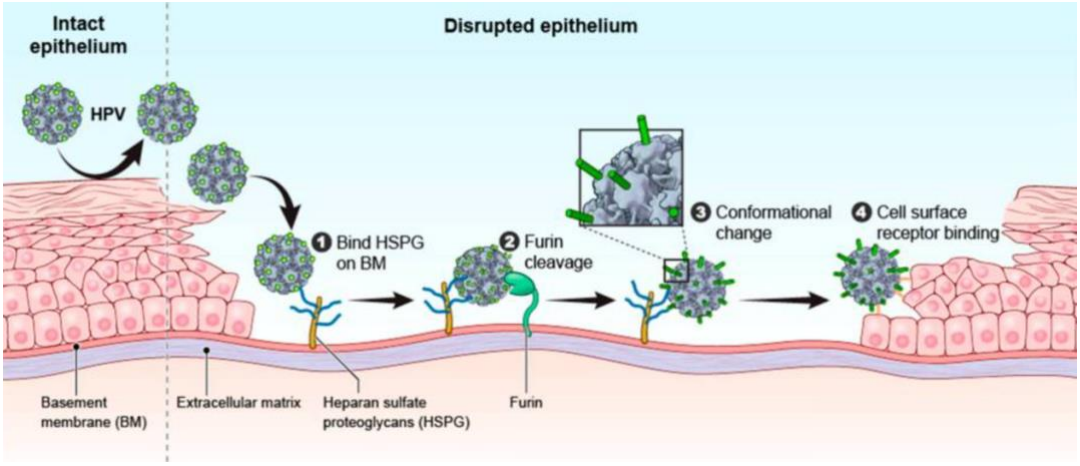

Figure 3. HPV attaches to HSPG on the exposed basement membrane. L2 protein is then cleaved by the action of a furin protease (2), resulting in a conformational change of the virion (3). Thereafter, the virion can bind to cell surface receptors (4) (Kines & Schiller, 2022).

Following infection and uncoating, the initial genome amplification phase starts in the basal keratinocytes of the epithelium. E1 and E2, among the first viral proteins to be transcribed, are necessary in this process to maintain the episomal genome at low copy number (50-200 copies per cell) (Gheit, 2019). E2 protein contains a DNA-binding domain and a protein-binding domain. As homodimer, it can bind to four palindromic sites in the LCR, three of which are adjacent to the origin of replication and are required for E1-activated viral replication. In addition, E2 can interact with E1 that binds the ori, resulting in the recruitment of the cellular DNA replication machinery (Graham, 2017; McBride, 2013). E2 acts also in limiting the expression levels of the early proteins by transcriptionally repressing the P97 promoter to avoid the activation of the immune response; therefore, HPV is capable in maintaining infection of epithelial cells over a significant period (Graham, 2017).

In normal epithelium, basal cells exit the cell cycle soon after migrating into the suprabasal cell layers and undergo a process of terminal differentiation. Conversely, in HPV-infected cells, the virus has developed strategies to prevent cell cycle arrest and apoptosis signals. Here, a key role is played by the oncoproteins E6 and E7, which inactivate tumor suppressor proteins and activate signal transduction to ensure that the infected cells remain proliferating and progress

to the S phase (Gheit, 2019). Furthermore, E7 protein is involved in the activation of another crucial pathway for the HPV genome amplification upon differentiation: the DNA damage response pathway, mainly ATM signaling pathway (Graham, 2017; Hong & Laimins, 2013). These are important steps for the establishment of the second - productive - phase of viral genome replication that occurs in cells of the mid to upper epithelial layers. E4 and E5 proteins contribute to the efficient and productive replication by modifying the cellular environment (Doorbar et al., 2012).

The expression of the late proteins L1 and L2 and the following encapsidation of newly replicated genomes represent the completion of the viral life cycle. Virion assembly occurs in terminally differentiated keratinocytes and fully formed virions are released through dead squames that are shed from the epithelial surface (Gheit, 2019; Graham, 2017; Harden & Munger, 2017).

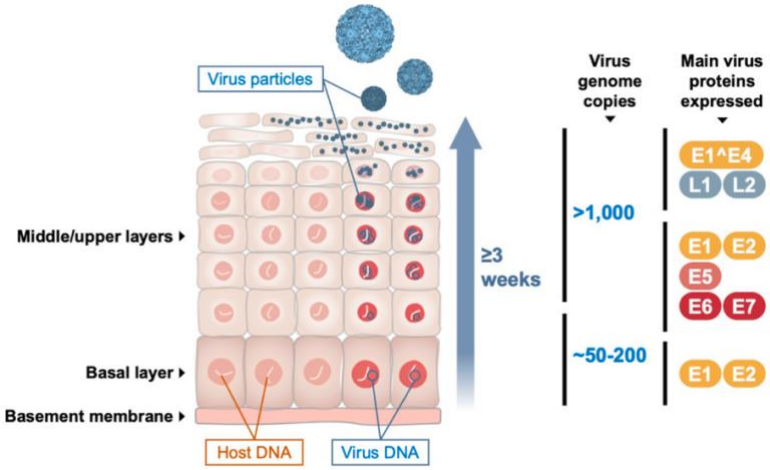

Figure 4. Infection is thought to require a microtear exposing the basal layer of the epithelium, where host cells susceptible to infection reside. In around 3 weeks viral genome copy number increases from reservoir levels by at least an order of magnitude. Different viral proteins dominate expression at different levels of the epithelium, in coordination with host cell differentiation. Viral particle formation takes place only in the upper layers, where the capsid proteins L1 and L2 are expressed. (Nelson & Mirabello, 2023).

2.1.4 HPV life cycle deregulation and cancer progression

The ordered expression of viral gene products that leads to virus particle production is lost in HPV-associated neoplasia (Doorbar et al., 2012). Although the hrHPV infection is associated with human cancers, the progression to cervical cancer is a rare event and results after a long latency period (zur Hausen, 1996). A major role is played by E6 and E7 proteins, whose dysregulated expression is often (~70-80% of the cases) due to the integration of the viral

genome into the host genome, resulting in a disruption of E2 coding sequence. The overexpression of the viral E6 and E7 oncogenes promotes cellular proliferation, abrogates cell cycle checkpoints, and causes progressive genetic instability, giving cells a selective growth advantage and driving oncogenic transformation. HPV integration events can be detected in cervical premalignant lesions that are known as cervical intraepithelial neoplasia (CIN) (McBride & Warburton, 2017). CINs are graded into three progressive groups based on the proportion of abnormally affected epithelium: CIN 1, CIN 2, and CIN 3. CIN 1 are low-grade cervical abnormalities (low-grade squamous intraepithelial lesions – LSIL) and are usually cleared by the immune system within one year. On the other hand, CIN 2 and CIN 3 are high-grade cervical abnormalities (high-grade squamous intraepithelial lesions – HSIL) and have an escalated risk for cervical cancer progression. An accurate identification of the lesion grade has also a prognostic significance, as around 20% of CIN 1 will progress to CIN 2, and around 30% of CIN 2 will progress to CIN 3, when untreated. CIN 3 are generally considered the direct precursors of cervical cancer, and around 40% of CIN 3 lesions will progress to cervical cancer in the absence of intervention (Burd, 2003; Zhou et al., 2019). In addition, the expression of E6 and E7 proteins increases from CIN 1 to CIN 3 lesions, reflecting the neoplastic phenotype. In CIN 1 lesions, the ability to complete the HPV life cycle and to produce viral particles is retained, whereas in CIN 2+ lesions the elevated level of E6 and E7 predisposes cells to genetic errors accumulation and, consequently, to cancer progression (Doorbar et al., 2012).

Although the continuous expression of these proteins is required to maintain the transformed phenotype, it is not sufficient for virus-mediated carcinogenesis (Graham, 2017); about the 90% of healthy individuals are capable to successfully clear HPV lesions within 1-2 years. HPV infection activates a cell-mediated immune response that results in T cell infiltration and, from 6 to 12 months after infection, in anti-HPV antibodies production (McBride, 2022). As it has been observed in studies using animal models, lesion regression, rather than occurring through massive apoptosis or cell death, the infected cells are actively replaced with apparently normal cells that still contain viral genomes with very low viral gene expression (Doorbar et al., 2012). Latent infections most likely take place in dividing stem cells where the virus can persist with very tiny gene expression. Given that, HPV latent infection emerges as an important feature in the establishment of persistent infection.

Therefore, to achieve a persistent infection that will progress to cancer, HPVs have evolved mechanisms to inhibit interferons production, JAK-STAT pathway-dependent transcription factors, and to evade immune system (Hong & Laimins, 2013).

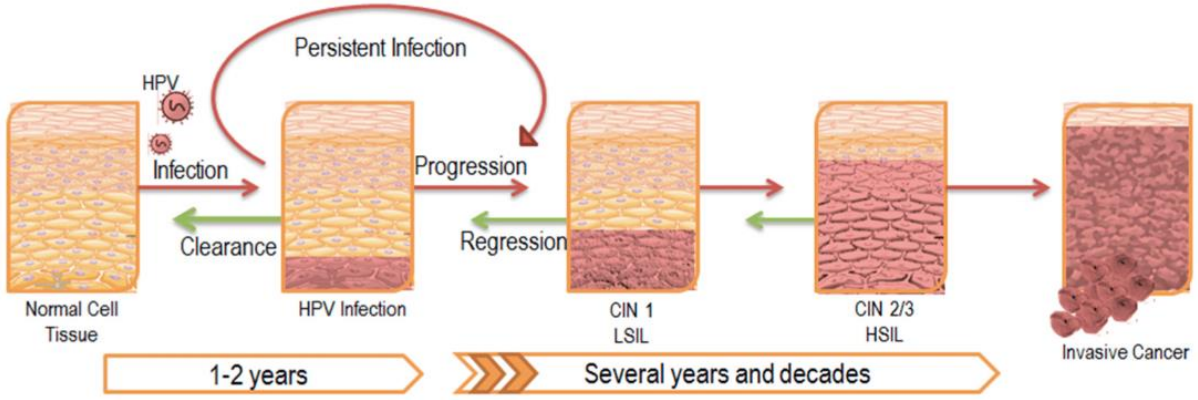

Figure 5. Most of the HPV infections are transient and are cleared by the immune system within a couple of years. However, 10–20% of infections persist latently, leading to disease progression. Lesions are known as cervical intraepithelial neoplasia (CIN) and are classified according to its severity. Low-grade squamous intraepithelial lesions (LSIL) advance to high-grade squamous intraepithelial lesions (HSIL), leading to invasive carcinoma. Despite tumor regression in response to initial treatment, most cases of latent infection prevent complete clearance of the viral infection and eventually results in lesion reoccurrence (Shanmugasundaram & You, 2017).

2.1.5 HPV-derived head and neck squamous carcinomas

Head and neck squamous cell carcinomas (HNSCCs) are a heterogeneous group of tumours arising in epithelial cells of mucosal linings of different anatomical sites of the upper aerodigestive tract, including paranasal sinuses, lips, oral cavity, pharynx (nasopharynx, oropharynx, hypopharynx), and larynx (Ghiani & Chiocca, 2022). HNSCCs have been correlated to alcohol consumption, smoking, and poor oral hygiene, and only more recently hrHPVs emerged as a risk-factor for the pathogenesis. As for cervical cancer, the most involved hrHPV is HPV16 (~90% of the cases). It is mainly associated with a subset of oropharyngeal squamous cell carcinomas (OPSCCs) arising from tonsillar crypts, the epithelium with the most susceptibility to cellular transformation in the head and neck region (Johnson et al., 2020; Sabatini & Chiocca, 2020). Thus, the incidence of HPV-positive OPSCC has significantly increased in the last decades and HPV is expected to become its major etiological factor by 2040 (Estêvão et al., 2019).

Despite their histological similarities, HPV-positive and HPV-negative HNSCCs are now considered as two distinct cancers, with different molecular profiles, tumour characteristics

and outcomes. HPV-positive HNSCCs are typified by p53 degradation, pRb down-regulation, and p16 upregulation. In these tumours, cancer progression is mediated by viral E6 and E7 oncoproteins or by genome integration-induced genomic rearrangements. By contrast, HPV-negative HNSCCs are characterized by p53 mutation, pRb upregulation, and p16 downregulation and cancer progression is mediated by alcohol and tobacco carcinogens-induced hyper mutational status and chromosomal instability (Ghiani & Chiocca, 2022; Powell et al., 2021). Furthermore, other quite common molecular features of HPV-positive HNSCC are EGFR amplification and PI3K/AKT/mTOR pathway aberrant activation (Sun et al., 2021). HPV status is also a prognostic marker. Indeed, HPV-positive OPSCC patients show a significantly improved overall and disease-free survival compared to HPV-negative OPSCC (e.g. NCT00047008 clinical trial (RTOG 0129) – 3 years overall survival (OS) 82,4% vs 57.1%; p<0.001) (Ang et al., 2010; Radiation Therapy Oncology Group, 2023).

Currently, traditional standard-of-care treatment for patients with localized or locally advanced OPSCC is combined cisplatin-based chemotherapy and radiation, excluding patients with early-stage disease who may be qualified for surgical intervention. That treatment has been shown to be very effective, with a 5-year OS of up to 95% in HPV-positive patients (You et al., 2019). Another possible therapeutic strategy can be the use of PI3K inhibitors that showed promising results but still have a long way to go (Sun et al., 2021).

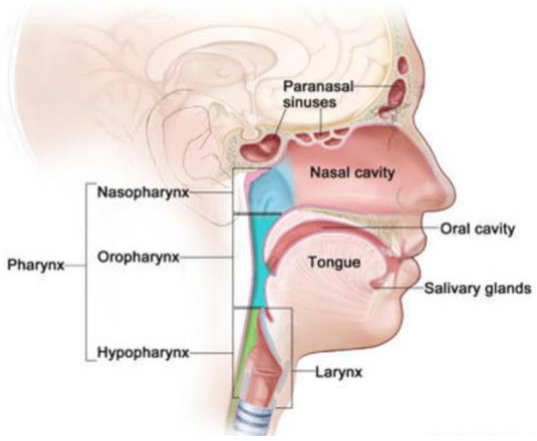

Figure 6. Head and neck cancer regions (National Cancer Institute)

2.2 SIRT1 AND CANCER

The mammalian Sirtuins (SIRT1-7) are NAD+-dependent class III histone deacetylases. During the deacetylation process NAD+ is hydrolysed and the lysine-bound acetyl group of their target proteins is transferred on APD-ribose with the formation of nicotinamide and 2'-O-acetyl-ADP-

ribose (Wu et al., 2022). Sirtuins have different subcellular localization and a high number of both histone and non-histone targets (Roth & Chen, 2014). SIRT1 is the most studied Sirtuin and it is involved in the regulation of different important cellular processes including cell proliferation, apoptosis, cell invasion and metastasis, inflammation, oxidative stress, glucose and lipids metabolism, autophagy, aging, genetic stability, and DNA repair (T. F. Liu & McCall, 2013; Roth & Chen, 2014; Wu et al., 2022). As mentioned before, SIRT1 is involved in the deacetylation of histones, such as histone H4 lysine 16 (H4K16), histone H3 lysine 9 (H3K9) and 14 (H3K14), histone H1 lysine 26 (H1K26), and in the deposition of histone variants (e.g. γH2AX), leading to gene silencing and heterochromatin formation (Roth & Chen, 2014). SIRT1 also regulates histone methylation inducing the production of H4K20me, H3K9me3, and H3K79me2 (Vaquero et al., 2004). Moreover, SIRT1 recruits the histone methyltransferase SUV39H1 and deacetylases it on Lys266 in its catalytic SET domain to stimulate its methyltransferase activity, resulting in increased levels of the H3K9me3 modifications (Z. Li et al., 2009; Vaquero et al., 2007). However, the most relevant action of SIRT1 is that on non-histone substrates, such as p53, FOXO1 and 3, HIF1α, and NF-kB. SIRT1 directly interacts with and deacetylases p53 on Lys382 residue, which will be then ubiquitinated and degraded by the E3 ubiquitin ligase E6AP-E6 complex, leading to a decreased transcription factor activity at the promoter region of p21 and consequently to the inhibition of the p53-dependent apoptotic response (Luo et al., 2001; Vaziri et al., 2001). In addition, SIRT1 interacts with hypermethylated in cancer 1 (HIC1), a tumor suppressor and transcriptional repressor epigenetically inactivated in cancer, to form a transcriptional repression complex, which directly binds to SIRT1 promoter impairing its transcription. HIC1 depletion results in upregulated SIRT1 levels and reduced p53 function, allowing cells to bypass apoptosis and survive DNA damage, and therefore predisposing cells to cancer (Lin & Fang, 2013). For these reasons, SIRT1 upregulation has been described in many cancers, such as breast cancer (Y. Xu et al., 2018), non-small cell lung cancer (X. Li et al., 2018), hepatocellular carcinoma (L. Liu et al., 2016), colorectal cancer (Ren et al., 2017), prostate cancer (Huffman et al., 2007), cervical cancer (So et al., 2018), endometrial cancer (Asaka et al., 2015), glioma (H. Chen et al., 2019), and leukemia (F. Wang et al., 2021). In addition, elevated expression of SIRT1 in gynaecological tumours was found associated with chemotherapy and radiotherapy resistance and correlated with poor prognosis and survival (Velez-Perez et al., 2017). However, some evidence show that it can act as both oncogene and/or tumor suppressor depending on cellular contest, target,

cancer type, and stage (Wu et al., 2022). For example, in ovarian cancer SIRT1 reduces high mobility group box-1 (HMGB1) protein expression and acetylation inhibiting migration, invasion, and angiogenesis (Jiang et al., 2018). Furthermore, SIRT1 deacetylases also p65 subunits of NF-kB, blocking the transcription of its downstream anti-apoptotic genes (Lin & Fang, 2013; Roth & Chen, 2014). Finally, SIRT1 could have a potential role as diagnostic and prognostic biomarker in patients with cancer (Wu et al., 2022).

2.2.1 SIRT1 in HPV-associated cancer

Cervical cancer represents the last step of progressive cervical disease. As described above, hrHPV E6 and E7 proteins are the major responsible for HPV-driven carcinogenesis, and higher levels of SIRT1 have been determined in this malignancy. However, few is known about a possible relationship between the virus and SIRT1.

Being a critical regulator of both basal viral replication and transcription, SIRT1 has been reported to play an important role in modulating HPV life cycle. It interacts with HPV31 genome modifying the acetylation status of URR-bound histones H1 (Lys26) and H4 (Lys16) and controlling the recruitment of some members of the ATM DNA damage response pathway (e.g. NBS1 and Rad51) (Langsfeld et al., 2015). Furthermore, Das and colleagues found that SIRT1 is a member of the HPV16 E1-E2 DNA replication complex and is recruited to the viral origin of replication in an E1-E2-dependent manner (D. Das et al., 2017). In line with the study of Langsfeld, Das and colleagues hypothesised that HPV requires SIRT1-dependent recruitment of homologous recombination factors (i.e. NBS1 and Rad51) to amplify its genome in undifferentiated cells as well as in the uppermost layers of the infected epithelium.

Allison and colleagues reported that SIRT1 is upregulated by HPV16 E7 oncoprotein in human cervical cancer SiHa cell line (Allison et al., 2009), but it remains unclear whether they directly interact each other. In this work, the authors demonstrated that HPV16 E7 influences SIRT1 levels by acting at post-transcriptional level and confers a pro-survival effect to cervical cancer cells. In particular, RNAi-mediated silencing of HPV E7 in SiHa cells reduces SIRT1 protein levels by ~50% 48 hours post-transfection and induces apoptosis. Similar results were obtained also in primary human keratinocytes transfected with HPV E7 expression vector (Allison et al., 2009). These results are consistent with and may explain to the overexpression of SIRT1 protein in CINs and squamous cell carcinomas (SCCs), as revealed by Velez-Perez and colleagues (Velez-Perez et al., 2017). The authors evaluated the expression of the protein in

101 tissue specimens from uterine cervix including 28 CIN 1, 32 CIN 2, 16 CIN 3, 2 microinvasive SCC, and 22 invasive SCC. 13,8% of CIN 1, 40,6% of CIN 2 and 50% of CIN 3 showed SIRT1 overexpression prevalently at cytoplasmic level. On the other hand, 68% of SCC showed SIRT1 overexpression at both nuclear and cytoplasmic level, 25% of SCC only at cytoplasmic level, and 4% of SCC only at nuclear level (Velez-Perez et al., 2017). These results indicate that increasing expression of SIRT1 is positively correlated with the progression of cervical disease. In addition, in the laboratory of Molecular Virology headed by Professor Gariglio, the group I joined for my internship, it has been demonstrated for the first time the role of SIRT1 in HPV-driven carcinogenesis. Indeed, they revealed the existence of a novel SIRT1-dependent circuit whose disruption leads to restoration of a functional p53 in HPV-transformed cells. Specifically, they found that SIRT1 inhibition, either by the specific pharmacological inhibitor EX527 (also known as Selisistat) or gene silencing, leads to K382-acetylated p53 restoration in HPV-transformed cells. Consistently, EX527 treatment promotes cell cycle arrest in G_0/G_1 phase and reduces cell viability and clonogenicity of HPV^+ cells, but not of HPV^- cells. Moreover, they demonstrated that SIRT1 inhibition increases the sensitivity of HPV^+ cells to sublethal doses of standard genotoxic agents, such as doxorubicin and cisplatin (Lo Cigno et al., 2023).

2.3 MINICHROMOSOME MAINTENANCE COMPLEX

DNA replication is a crucial event of the cell cycle. Indeed, the initiation of chromosome replication in eukaryotic cells is strictly regulated to ensure the production of a single copy of the DNA in each cell cycle. The assembly of Cdc45-MCM-GINS helicase is the key regulated step of this process (Xia et al., 2023). Although well characterized in *Saccharomyces Cerevisiae* and *Xenopus laevis*, DNA replication system is highly conserved across all eukaryotes (Ying & Gautier, 2005). Among the different protein complexes recruited to the DNA during replication, there is the minichromosome maintenance (MCM) complex, which consists of six proteins (MCM2, 3, 4, 5, 6, 7 – briefly MCM2-7) arranged in a ring-shaped hexamer (Meagher et al., 2019). MCM2-7 proteins belong to the AAA+ ATPase (ATPases associated with a variety of cellular activities) superfamily and are required for both initiation and elongation during DNA replication (Drissi et al., 2018). Their activities are organised in a defined sequence of recruitment, loading, and activation, following the two different steps in which DNA replication can be divided into. Firstly, during G1 phase of the cell cycle two MCM complexes assemble head-to-head with Cdc6 and Cdt1 at replication origins to form the pre-replication complex

(pre-RC). This step needs ATP hydrolysis and allows the loading of MCM2-7 proteins onto the double strand of the DNA (Bochman & Schwacha, 2009; Meagher et al., 2019). Secondly, immediately after entering the S phase, cyclin- and Dbf4-dependent kinases (CDKs and DDKs) activity promotes the recruitment of Cdc45 and GINS resulting in the formation of an active helicase complex, the Cdc45-MCM-GINS (CMG) complex (Bochman & Schwacha, 2009; Meagher et al., 2019). CMG complex is involved in DNA unwinding (replication forks) and subsequent recruitment of the replication machinery, including DNA polymerases and other factors that participate in the assembly of the replisome complex (Neves & Kwok, 2017). Surprisingly, helicase activity of the CMG complex is provided by MCM complex, even though MCM2-7 proteins alone do not show any DNA helicase activity (Masai et al., 2010). Upon initiation of DNA replication in S phase, they start moving from replication origins. In response to the binding of Cdc45, GINS and all the other "firing factors", MCM complexes undergo separation and remodelling so that each MCM hexamer encircles a single DNA strand (Abid Ali et al., 2016; Douglas et al., 2018).

When two progressive replication forks converge, DNA replication machinery must be inhibited to prevent over-replication. A main role in the termination phase is played by the E3 ubiquitin ligase $CRL2^{Lrr1}$ (Cullin RING ligase) that ubiquitinates MCM7 subunit and recruits p97, which dissociate the CMG complex from the DNA (Dewar et al., 2017).

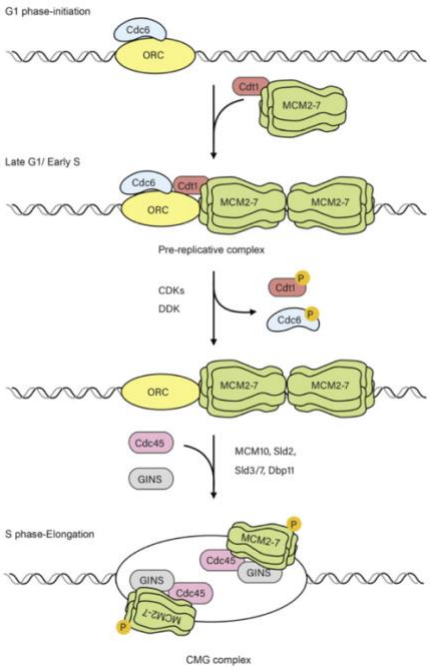

Figure 7: MCM involvement in eukaryotic DNA replication initiation and elongation. At the beginning of G1 phase, Cdc6 and Cdt1 recruit and load MCM2-7 to origins of replication to form the stable and inactive pre-RC. In late G1 phase, the pre-RC is somehow activated for DNA unwinding by CDKs and DDK. This facilitates

the loading of additional replication factors (e.g., Cdc45, Mcm10, GINS, and DNA polymerases) and unwinding of the DNA at the origin. During S phase, Cdc6 and Cdt1 are degraded or inactivated to block additional pre-RC formation, and bidirectional DNA replication ensues (Bochman & Schwacha, 2009; Y. Wang et al., 2020).

MCM2-7 proteins play a main role in DNA replication increasing proliferation, therefore an association with cancer is not surprising. Indeed, it is well known that these proteins contribute to tumor initiation, progression, invasion, metastasis via affecting epithelial to mesenchymal transition, and angiogenesis (Stewart et al., 2017; J. Xu et al., 2006). For these reasons, an aberrant expression and activation of these proteins were frequently found in many premalignant lesions and malignancies, leading to genome instability and uncontrolled cell cycle progression (Figure 8) (Y. Wang et al., 2020). Indeed, the MCM proteins are often positively related with Ki67, a well-known proliferation marker, in tumors (Neves & Kwok, 2017; Y. Wang et al., 2020). Furthermore, MCM overexpression is correlated with poor prognosis in cancer patients. For example, MCM2 is correlated with reduced OS in lung and liver cancer and with reduced OS and disease-free survival (DFS) in gastric cancer (Y. Wang et al., 2020). Instead, MCM7 is correlated with relapse and invasion in prostate cancer, with poor survival rate in oesophageal squamous cell carcinoma (Neves & Kwok, 2017), and with reduced OS in non-small cell lung cancer (Toyokawa et al., 2011). This evidence suggests that MCM2-7 proteins can represent a reliable prognostic marker and even a possible therapeutical target for the treatment of this type of cancer as their depletion or downregulation results in reduced cellular growth.

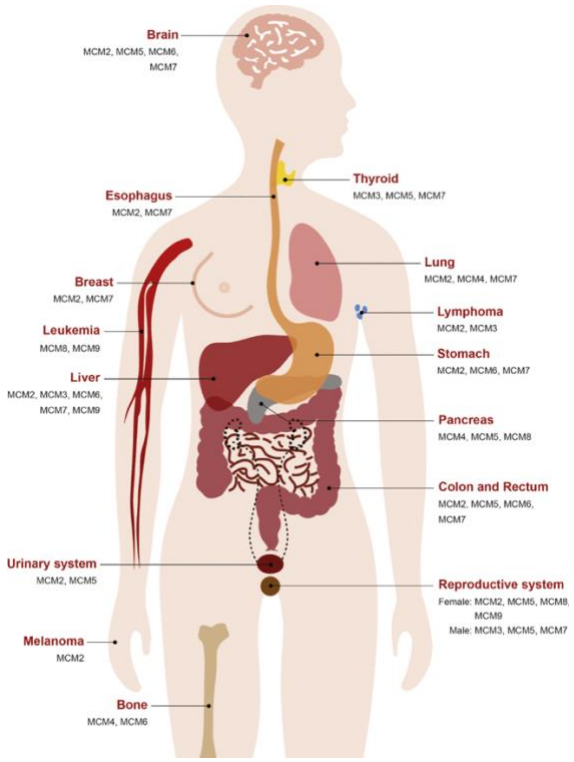

Figure 8. Aberrant MCM activation in different cancer types (Y. Wang et al., 2020)

2.3.1 MCM7 in HPV carcinogenesis

MCM7, one of the MCM complex component that binds to DNA double strand at replication origins in the late G1 phase and forms the pre-RC complex during cell cycle progression, is highly expressed in various cancers and can be used as a potential proliferation marker. This scenario can also be applied to HPV-driven oncogenesis where MCM7 upregulation has been steadily observed in both *in vitro* and *in vivo* setting, including human cancers, being considered an informative biomarker of E6/E7 deregulation and ensuing oncogenic activity. Indeed, MCM7 was found significantly upregulated in cervical cancer, CIN precursor lesions, and in *in vitro* organotypic raft cultures of human cervical keratinocytes harbouring HPV16 genome (Brake et al., 2003; M. Das et al., 2013; Kang et al., 2018). In particular, MCM7 represents a highly informative marker for the progressive disease that leads to cervical cancer. Indeed, Brake and colleagues demonstrated that increased MCM7 expression was observed in cervical cancer samples and HSILs arising from oestrogen-treated transgenic mice with HPV16 E7 protein or with both HPV16 E6 and E7 proteins expressed in the basal layer of the epidermis. Conversely, in LSILs and hyperplastic cervical epithelium from non-transgenic mice and transgenic mice with HPV16 E6 protein expressed in the basal layer of the epidermidis, MCM7 expression was lower and restricted to basal and parabasal layers. Similar results were found

even in biopsies from patients with progressive cervical disease (Brake et al., 2003). Moreover, it was demonstrated that deregulated MCM7 expression in the epidermis strongly influences both incidence and prevalence of papilloma formation as well as the progression from papilloma to squamous cell carcinoma (SCC) (Honeycutt et al., 2006).

The upregulation of MCM7 in HPV-positive tumors was demonstrated to be due to E7 as a consequence of the pRB inactivation as it is an E2F-responsive gene (Balsitis et al., 2006). Indeed, by binding and consequently inactivating pRb, E7 activates the E2F family of transcription factors enabling the expression of E2F-responsive genes (Brake et al., 2003).

In addition, MCM7 is known to interact with hrHPV E6 through its C-terminal domain (Kukimoto et al., 1998) and with E6AP via a homotypic motif called L2G box (Kühne & Banks, 1998). In particular, Kühne and Banks demonstrated that MCM7 turnover is mediated by E6AP ubiquitination, suggesting a potential role of MCM7 as an E6AP-regulated checkpoint for DNA licensing that is irreversibly degraded after successful initiation of the DNA replication (Kühne & Banks, 1998).

Some studies reported that MCM2-7 proteins may interact with the deacetylase SIRT1. In particular, it was conducted a proteomic study in 293T cells transfected with Flag-SIRT1 plasmid and it was demonstrated that SIRT1 interacts with three components of the MCM complex, i.e. MCM3, 5, and 7 suggesting a possible role of these deacetylase in DNA replication origin firing (R.-H. Wang et al., 2014). In addition, it was found that the acetylation levels of the MCM proteins are significantly increased in SIRT1 knockout (KO) MEF cells. Specifically, acetylation of K857 and K818 on MCM4 increased by at least 40% upon SIRT1 knockout, and one acetylation site (K173) on MCM6 was identified only in SIRT1 knockout cells (Y. Chen et al., 2012). Lastly, Thakur and colleagues identified MCM proteins as binding partners for SIRT1 on chromatin in HCT116 cells harbouring WT or mutant SIRT1 by performing SIRT1 chromatin interactome analysis using mass-spectrometry. Moreover, co-immunoprecipitation of the active phosphorylated SIRT1 (pT530-SIRT1) revealed interactions of pT530-SIRT1 with MCM2, MCM4, MCM6, and MCM7 and these proteins was found acetylated in KO or mutant SIRT1 cells but not in WT cells (Thakur et al., 2022).

3. OBJECTIVE OF THE THESIS

Recently, the group I joined for my internship has demonstrated the role of the cellular deacetylase SIRT1 in the carcinogenesis driven by HPV in epithelial cells and the potential of SIRT1 inactivation as a cornerstone of novel therapeutic strategies in preclinical models. Indeed, they demonstrated that SIRT1 upregulation is crucial for p53 deacetylation and its ensuing destabilization (or degradation), thus providing an alternative, attractive, and feasible option to inhibit cancer cell proliferation by using the specific pharmacological inhibitor of SIRT1 EX527. In this context, we propose to better understand the role of SIRT1 in HPV-induced carcinogenesis in more physiological systems like NOKE6/E7 organotypic raft cultures and a NOKE6/E7-based allogeneic HPV16-induced mouse cancer model and to assess whether targeting this protein could be an effective strategy for the treatment of HPV-associated cancer. Moreover, to shed light on the molecular mechanism underlying SIRT1 involvement in HPV-driven cancers, we aim to identify SIRT1 interacting partners in NOKE6/E7 cells using a proteomic approach. A mass spectrometry analysis on protein extracts from NOKE6/E7 cells co-immunoprecipitated for SIRT1 revealed a network of interacting proteins involved in DNA replication, such as MCM7 and MCM4. In this work, we propose to validate their interaction with SIRT1, supporting the hypothesis about the existence of a DNA-binding platform comprising SIRT1 and the MCM complex at the replication origin necessary to prevent excess replication and preserve genomic stability.

4. MATERIALS AND METHODS

4.1 Cell culture and treatments

HFF (human foreskin fibroblasts) were cultured in DMEM medium (Sigma-Aldrich) supplemented with 10% fetal bovine serum (FBS; Sigma-Aldrich), 100 U/mL penicillin, 100 µg/mL of streptomycin and 0.05% mM glutamine. NOKs HPV16 E6/E7 (for brevity NOKE6/E7), normal oral keratinocytes stably transduced with both E6 and E7 genes of HPV16 by lentiviral transduction, and their control counterpart (NOK, transduced with an empty control vector) were grown in keratinocyte serum-free medium (KSFM) supplemented with 25 µg/mL bovine pituitary extract (BPE), 0.2 ng/mL recombinant epidermal growth factor (rEGF), 0.3 mM $CaCl_2$, 100 U/mL penicillin and 100 µg/mL of streptomycin. A highly expressing E6 and E7 clone with high proliferation rates was isolated from a pool of NOKE6/E7 cells by limiting dilution.

4.2 Organotypic raft cultures

Organotypic raft culture were generated as described by Wilson and Laimins (Wilson & Laimins, 2005). Specifically, keratinocytes are plated onto a dermal equivalent layer composted of rat tail type I collagen and HFF. To prepare dermal equivalent layer, transwell inserts were loaded in deep well plate and 1 mL of type I collagen pre-mix – containing type I collagen, F12 medium, 10% FBS, 1% penicillin and streptomycin, and 18,4 mM NaOH – is poured and incubated for 30 minutes at 37°C in a 5% CO_2 environment for jellification. $6x10^6$ HFF were then added to the remaining collagen pre-mix and dispensed at 2.6 mL per well into transwell inserts. Then, 18 mL of HFF media were added to the outer well and the plate was incubated at 37°C. After 4 days (day 0), 200µL ($1,5 \times 10^6$ cells) of NOKE6/E7 cells were plated onto each dermal equivalent. After 2 hours of incubation at 37°C, 19 mL of F-Medium Incomplete supplemented with 0.5% FBS (F-medium incomplete is composed by 3 parts of DMEM high glucose and 1 part of Ham's F12 medium and supplemented with 100 U/mL penicillin, 100 µg/mL of streptomycin, 0.4 ug/mL hydrocortisone, 85 ng/mL cholera toxin, 5 ug/mL insulin, 24.2 ug/mL adenine, and 1.88 mM $CaCl_2$) were added in the outer well. At day 4 from keratinocytes plating, transwell inserts were lifted by adding sterile cotton pads above them into each well, to re-create the air-liquid interphase. Every two days from seeding, the media in the outer well was changed and starting from day 4, 12 mL of Cornification Media were added (F-medium supplemented with 5% of FBS). To allow cells to be exposed to air and fed only from the bottom through cotton pads, the volume of the media in the outer well was reduced to 9 mL starting from day 6. At day 12 and 14 raft cultures were treated with EX527

(80 µM) or equal volume of DMSO and the day after incubated overnight with 20 µM of EdU (5-ethynyl-2'-deoxyuridine). At day 16 raft cultures were harvested. After removing the media from the outer well, the raft cultures were removed from each transwell insert by cutting the bottom of the well with a scalpel, turned down in a gauze, inserted in a tissue-tek cassette and incubated overnight in 10% buffered formalin solution. Lastly, dehydration and inclusion in paraffin was performed to obtain formalin-fixed paraffin-embedded (FFPE) samples.

4.3 Immunohistochemistry and Immunofluorescence

FFPE sections were deparaffinized by heating (56°C) for 30 to 60 minutes, then washed in xylene twice (2 x 15 minutes), re-hydrated through a graded series of ethanol washes (100%, 95%, 90%, and 75%), rinsed in PBS and treated with 3% hydrogen peroxide for 8 minutes in dark conditions to block endogenous peroxidase activity. After washing with PBS, antigens were retrieved using citric acid-based antigen unmasking solution (H-3300, Vector Laboratories, Newark, CA, USA) in a pressure cooker (Bio SB, Santa Barbara, CA, USA) according to manufacturer's instructions (15 minutes, High Pressure program) and then chilled to cool at room temperature for additional 30 to 40 minutes. Sections were rinsed in PBS and blocked with animal free Blocker and Diluent solution (SP-5035, Vector Laboratories, Burlingame, CA, USA) for immunohistochemical staining or with 10% normal goat serum (NGS) (S-1000, Vector Laboratories, Newark, CA, USA) for immunofluorescence staining for 1 hour at room temperature. Primary antibodies were diluted in blocking solution before being applied to the sections and incubated overnight at 4°C in a humidified chamber. The following antibodies were used: anti-p53 (sc-126, Santa Cruz Biotechnology, diluted 1:100), anti-Ki67 (ab16667, Abcam, diluted 1:200), anti-MCM7 (ab96849, Abcam, diluted 1:200). For EdU detection, before adding primary antibody a Click-iT reaction was performed accordingly to manufacturer's instruction (BCK-EdU488IM100, BaseClick GmbH). Briefly, slides were incubated for 30 minutes at dark with a reaction cocktail containing 10% of Reaction buffer, Reactor system, 1 mM of dye azide, and 10% of Buffer additive provided by the kit. The day after, sections for immunohistochemistry were washed in PBS and incubated with biotinylated horse anti-mouse/rabbit IgG (BP-1400, Vector Laboratories, Newark, CA, USA) for 30 minutes at room temperature. After washing in PBS 0.1% Tween-20, sections were incubated with Vectastain elite peroxidase reagent (PK-7100, Vector Laboratories, Burlingame, CA, USA) for 30 minutes at room temperature. Subsequently, sections were washed in 0.1% Tween-20 and

biotin signal was amplified by adding peroxidase DAB substrate kit (PK-4100, Vector Laboratories, Burlingame, CA, USA). Section counterstaining was performed using Haematoxylin for 30 seconds. Sections were dehydrated through a graded series of ethanol (75%, 95%, and 100%), cleared in xylene, and then mounted using Vectamount permanent mounting medium (H-5000, Vector Laboratories, Burlingame, CA, USA). Images were acquired with Axioscan 7 (Zeiss) and quantitated using QuPath software.

In contrast, after overnight incubation with primary antibody, sections for immunofluorescence were washed with PBS 0.05% Tween-20 and incubated with the respective species-specific Alexa Fluor 488-conjugated or Alexa Fluor 568-conjugated secondary antibody (Invitrogen) and DAPI (Invitrogen, diluted 1:600) for 1 hour in dark conditions at room temperature. Lastly, slides were mounted using SlowFade™ Gold antifade reagent (S36936, Invitrogen). Images were acquired with Axioscan 7 (Zeiss) and quantitated using QuPath software. For the assessment of histological features, the slides were stained with Haematoxylin and Eosin.

4.4 Protein extraction and quantification

Whole-cell protein extracts were obtained by adding in a 10 cm tissue culture dish cell lysis buffer containing 20 mM Tris-HCl pH 7.5, 250 mM NaCl, 1 mM EDTA, 1mM EGTA, 1% Triton X-100, 1mM DTT with the addition of protease (25 µL/mL, Sigma-Aldrich) and phosphatase inhibitors (10 µL/mL, Active Motif). After 5 minutes of incubation on ice, samples were scraped and sonicated (4 cycles of 5 seconds every 20 seconds). Then, samples were centrifuged at 16000 g for 10 minutes at 4°C. The supernatant containing soluble proteins was collected in a clean, low protein binding micro-centrifuge tube and quantified.

Protein concentration was determined using Bradford Protein Assay based on an absorbance shift of the dye Coomassie Brilliant Blue G-250. In an acidic environment, the red form of the dye is converted into its blue form, binding to the protein being assayed. The protein-dye complex causes a spectral shift in the absorption maximum of the dye from 465 to 595 nm. The increase of absorbance at 595 nm is proportional to the amount of bound dye, and thus to the amount (concentration) of protein present in the sample. Bovine serum albumin (BSA) was used to calibrate the assay by preparing six serial dilutions of protein diluted with PBS1X to final concentrations of 0, 1, 2, 4, 6, 8 µg/µl. The unknown sample was prepared by adding 2 µl of sample in the final volume of 498 µl of PBS1X. For each test tube 500 µl of Bradford

Reagent (Sigma-Aldrich) was added. Absorbance readings were measured at 595 nm using a spectrophotometer and a standard curve was plotted and used to provide a relative measurement of protein concentration of each sample.

4.5 Immunoprecipitation

NOKE6/E7 cells were plated in 10 cm tissue culture dish and 16 h before collecting cells medium was changed to boost cell growth. 300 ug of whole-cell protein extracts were incubated with the antibody for 1 hour at room temperature on a rotating mixer. The following antibodies were used: anti-SIRT1 (ab32441, Abcam), anti-MCM7 (ab96849, Abcam), anti-MCM4 (PA5-29039, Thermo Fisher Scientific), and control IgG (Diagenode). Next, immunocomplexes were incubated for 3 h with beads (Pierce Protein G agarose) that were previously washed in PBS and once in lysis buffer by centrifugation at 2000 rpm for 5 minutes at 4°C. Subsequently, immunocomplexes were washed, eluted in Laemmli Sample Buffer containing 1% bromophenol blue and 1% β-mercaptoethanol, heated at 95 °C for 5 minutes, and loaded on ReadyGels (7.5%, Bio-Rad) for immunoblotting.

4.6 Immunoblotting

Whole-cell protein extracts and immunocomplexes were separated by their molecular weight under denaturing conditions using ReadyGels. Samples, together with a molecular weight ladder, were loaded into appropriate wells, and the gel was run at 300V. Proteins were transferred from the SDS-polyacrylamide gel to nitrocellulose membrane by using Trans-Blot Turbo Blotting System according to manufacturer's instructions (Bio-Rad). To confirm the transfer, membranes were stained with Ponceau stain. To visualize the proteins, membranes were briefly washed with water and then three times by using TBS-T 1X (10mM Tris-HCl, pH 7.5, 100mM NaCl, 0.1% Tween-20). To minimize any unspecific interaction of the antibody with the membrane, it was blocked in 10% non-fat dry milk dissolved in TBS-T 1X for 1 hour. Next, membranes were incubated with primary antibodies overnight at 4°C on a rocker. The following antibodies were used: mouse monoclonal antibodies (MAb) anti-SIRT1 (ab110304, Abcam, diluted 1:1000) and anti-MCM7 (MA5-14291, Thermo Fisher Scientific, diluted 1:200), and rabbit polyclonal anti-MCM4 (PA5-29039, Thermo Fisher Scientific, diluted 1:800). Thereafter, membranes were washed 3 times in TBS-T 1X to eliminate unbound antibody residues and incubated with sheep anti-mouse secondary antibody (NA931, GE Healthcare) or

TidyBlot Western Blot Detection Reagent (STAR209PA, Bio-Rad) conjugated to horseradish peroxidase (HRP). Secondary antibodies are diluted in TBS-T 1X. Protein bands were visualized by enhanced chemiluminescence (34580, Super Signal West Pico, Thermo Fisher Scientific) using the instrument ChemiDoc Touch Imaging System (Bio-Rad).

4.7 Proximity Ligation Assay (PLA)

Protein-protein interactions were detected with Duolink® in situ PLA (Sigma Aldrich) according to manufacturer's instruction. Briefly, NOK and NOKE6/E7 cells were seeded on glass coverslips in 24-well plate. Medium was changed to boost cell growth 24 hours post seeding and after 16 hours cells were fixed with 4% paraformaldehyde (PFA) for 10 minutes, permeabilized with 0.2% Triton-X100 in PBS for 20 minutes on ice and blocked with Duolink Blocking Solution for 1 hour at 37°C. Primary antibodies were diluted in Duolink Antibody Diluent before being applied to coverslips and incubated overnight at 4°C in a humidified chamber. The following antibody pairs were used: mouse anti-SIRT1 (ab110304, Abcam, diluted 1:200) and rabbit anti-MCM7 (ab96849, Abcam, diluted 1:200); mouse anti-SIRT1 and rabbit anti-MCM4 (PA5-29039, Thermo Fisher Scientific, diluted 1:200); mouse anti-MCM7 (MA5-14291, Thermo Fisher Scientific, diluted 1:200) and rabbit anti-MCM4. Next, coverslips were washed with Wash buffer A 1x and incubated with the anti-rabbit PLUS and anti-mouse MINUS PLA probes diluted 1:5 in Duolink Antibody Diluent for 1 hour at 37°C. Then, coverslips were incubated with a ligation solution (Ligase diluted 1:40 in Duolink Ligation buffer) for 30 minutes at 37°C and next, with an amplification solution (Polymerase diluted 1:80 in Amplification buffer) for 100 minutes at 37°C. Lastly, after two washes in Wash buffer B 1x and one in Wash buffer B 0.01%, nuclei were stained with DAPI (diluted 1:600 in PBS) for 30 minutes at room temperature. Coverslips were mounted using SlowFade™ Gold antifade reagent (S36936, Invitrogen). Images were acquired with confocal microscope and quantified using QuPath software.

4.8 Statistical analysis

All statistical tests were performed using Graph-Pad Prism version 8 for Windows (GraphPad Software). The data are presented as mean ± standard deviation (SD). For comparisons consisting of two groups, means were compared using two tailed Student’s t tests. Differences were considered statistically significant at a P value of < 0.05.

5. RESULTS

5.1 The antiproliferative activity of EX527 is retained in NOKE6/E7 organotypic raft cultures

Recently, the group I joined for my internship has demonstrated for the first time the role of SIRT1 in the development and maintenance of HPV-associated tumors. Specifically, they found that SIRT1 pharmacological inhibition, using EX527, or genetic silencing of SIRT1 in HPV+ cell lines leads to the reactivation of a transcriptionally active K382-acetylated p53, leading to cell cycle arrest at G0/G1 phase and reduction of cell survival and clonogenicity compared to HPV- cells, in particular in NOKE6/E7 cells (Lo Cigno et al., 2023). As previously described, these cells are normal oral keratinocytes transduced with a lentiviral vector which ensures equal expression of HPV16 E6 and E7 oncoproteins, thanks to a mRNA self-cleaving sequence (P2A) inserted between E7 and E6 sequences (Yang et al., 2019) (Figure 9A).

Based on these findings, the first aim of this thesis was to better understand the role of SIRT1 in HPV-induced carcinogenesis in a more physiological system like NOKE6/E7 organotypic raft cultures. This *in vitro* three-dimensional system recapitulates the structure of the stratified squamous epithelia and was generated and treated as detailed in the materials and methods section and represented in Figure 9B. Firstly, these cultures were stained with haematoxylin and eosin (H&E) in order to evaluate the histological features and we observed a significant reduction in the number of suprabasal layers in EX527-treated cultures when compared to vehicle-treated cultures (Figure 9C). Intriguingly, the capability of NOKE6/E7 cells to invade into the underneath dermal equivalent matrix that was well evident in the vehicle-treated rafts was almost abolished upon EX527 treatment and the irregular masses of epidermal cells that proliferated down in the dermal matrix were largely lost upon treatment (Figure 9C). Next, in order to confirm the antiproliferative effect of EX527 on raft cultures we performed an immunofluorescence staining for the proliferation marker MCM7 and Edu. Indeed, MCM7 is involved in the DNA replication (Neves & Kwok, 2017) and it has been found upregulated in different types of cancerous lesions (Neves & Kwok, 2017; Toyokawa et al., 2011). In the context of HPV, MCM7 overexpression strongly correlates with HPV-induced precancerous lesion progression (from LSIL to HSIL) and for this reason it is widely recognised as a proliferation marker for HPV-associated malignancies (Brake et al., 2003; M. Das et al., 2013). Instead, EdU is a thymidine analogue incorporated by proliferating cells into the newly synthesised DNA, which is detectable after tissue processing via click-chemistry reaction and fluorophore binding. Hence, this combined staining allows to determine how many cells are proliferating (MCM7 positive) and replicating their genome (EdU positive) at the same time.

As shown in Figures 9D, the number of EdU and MCM7 positive cells was reduced by around 10% and 15%, respectively, in EX527-treated raft cultures in comparison with their counterpart ($p<0.001$). Interestingly, some EdU negative cells remained MCM7 positive, and this is probably due to SIRT1 inhibition-induced mitotic stress.

Altogether, these results demonstrate that SIRT1 inhibition has an antiproliferative activity also in a more physiological three-dimensional system.

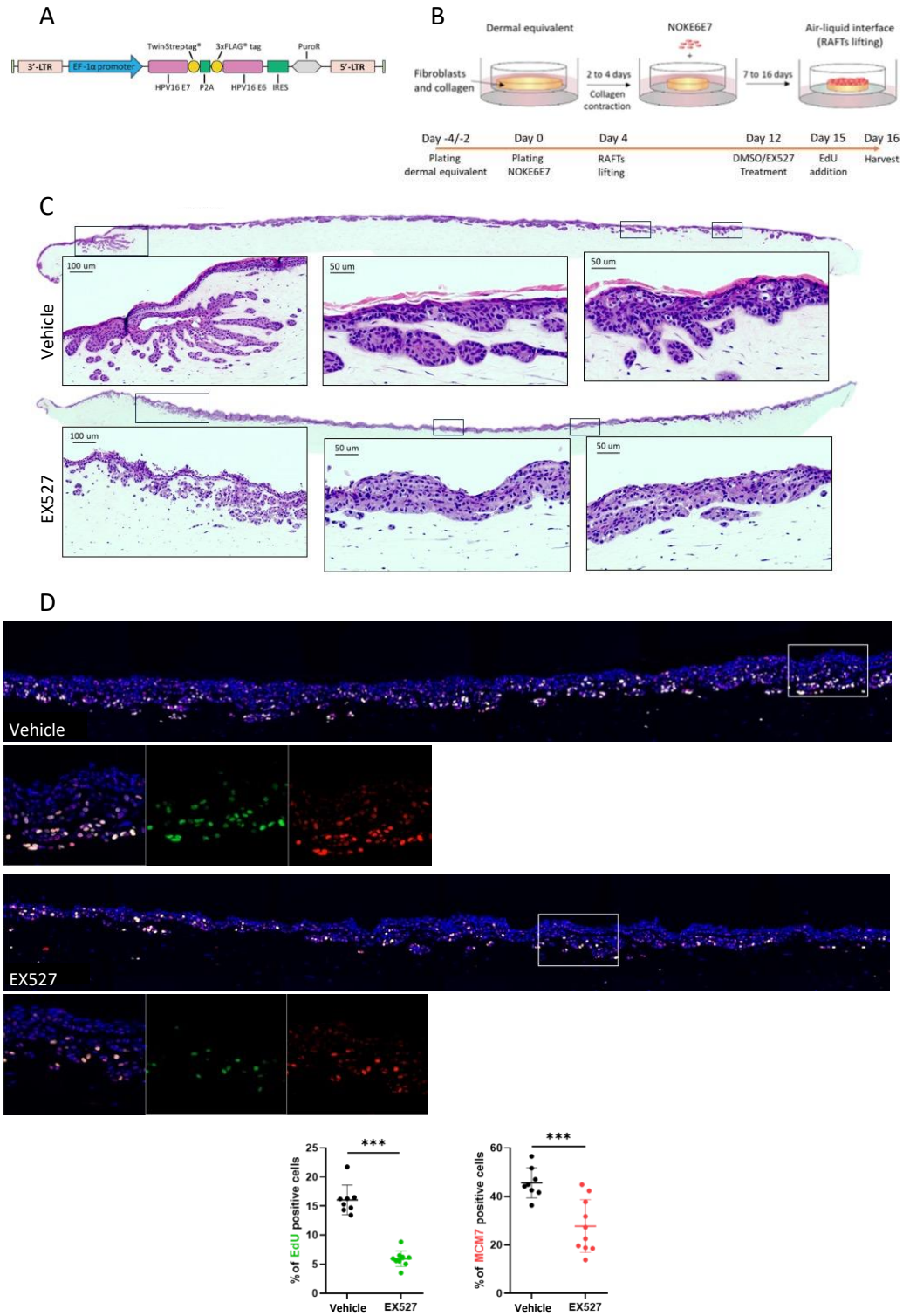

Figure 9. EX527 treatment reduces cell proliferation in NOKE6/E7 organotypic raft cultures. (A) Schematic representation of the lentiviral vector used to stably express E6 and E7 in immortalized normal oral keratinocytes (NOKs). (**B)** Schematic representation of the organotypic raft cultures experimental timeline. Briefly, Type I Collagen and HFF cells were plated in transwell inserts loaded in deep well plate 4 days before (day -4) plating NOKE6/E7 cells (day 0). Starting from day 12 every two days organotypic raft cultures were treated with EX527 or vehicle until harvesting (day 16). 24 hours before collecting, cells were incubated with EdU. **(C)** Representative images of H&E staining on NOKE6/E7 organotypic raft cultures treated with EX527 or vehicle. **(D)** Representative images of MCM7 (red) and EdU (green) immunofluorescence staining on organotypic raft cultures treated with EX527 or vehicle. The percentage of cells positive for MCM7 or EdU were quantified and plotted. Errors bars indicate SD. *** $p < 0.001$, unpaired T-test.

5.2 SIRT1 inhibition impacts on tumor burden in the allogeneic HPV16-induced mouse cancer model

The results described so far support the hypothesis that SIRT1 upregulation is a key mechanism of HPV-driven oncogenesis and that its inhibition affects HPV-transformed cell proliferation. Thus, to assess the therapeutic potential of SIRT1 inhibition, we moved in an *in vivo* model using a HPV16-induced xenograft mouse cancer model. To this end, 4-6 weeks old NOD SCID γ-null (NSG) mice were subcutaneously inoculated in the back with 10^6 NOKE6/E7 cells in a 1:1 volume ratio with Matrigel (Corning, 200 µL/mouse). After 10 days, when tumors become palpable and reach about 20 mm^3 in volume, intraperitoneal injections of vehicle or EX527 were performed every other day for a total of 6 doses. After 48h from the last administration, tumors were harvested and processed for subsequent histologic analyses (Figure 10A).

The tumor formation in the two groups of mice was assessed by measuring every other day the tumor volume and, when the animals were sacrificed, the tumor weight. As already reported in the syngeneic HPV16-driven mouse cancer model used by Lo Cigno and colleagues (Lo Cigno et al., 2023), SIRT1 inhibition underlies a tumor growth impairment in terms of tumor size and weight, when compared to vehicle-treated ones (Figures 10B, 10C). Next, to evaluate the histology of tumors, an H&E staining on FFPE sections was performed. Interestingly, we found that NOKE6/E7-derived tumors exhibited the same phenotypic characteristics of HPV-driven squamous cell carcinomas (SCC), showing high nuclear-to-cytoplasmic ratio, frequent mitosis, koilocytosis (HPV-mediated cytopathic effect), and the characteristic invasive growth pattern of HPV-associated SCC (Figure 10D). Furthermore, we observed that vehicle-treated samples showed a great number of mitotic cells and keratin pearls (Figure 10D, upper panel), indicating that cells were in a proliferative status. However, among the mitotic ones, some cells

(red circles – Figure 10D upper panel) present atypical mitosis with misaligned chromosomes at the metaphasic layer. Conversely, in EX527-treated tumors there is a dramatic reduction of mitotic cells, accompanied by an increase in apoptotic cells (yellow circles – Figure 10D, lower panel). In addition, the presence of multinucleated cells (red circles – Figure 10D lower panel) suggested that SIRT1 inhibition can result also in mitotic stress since cells replicate their genome but lose the ability to complete cytokinesis.

Subsequently, to determine whether the responsiveness of NOKE6/E7 to EX527 treatment *in vivo* also involved p53 restoration, tissue sections were stained for p53 expression by immunohistochemistry. A significantly increased number of p53-positive cells was found in mice treated with EX527 than those treated with vehicle (30% in control mice vs 60% in EX527 group) (Figure 10E). Lastly, to confirm the different mitotic phenotype observed in H&E-stained sections, we assessed the proliferation marker Ki67 by immunohistochemistry. Consistently with p53 restoration and the antiproliferative activity of EX527, the number of Ki67 positive cells was moderately reduced, but statistically significant, in samples from EX527-treated mice when compared to vehicle-treated ones (from 86% in vehicle-treatment group to 75% in EX527-treated mice) (Figure 10F.).

Altogether, these results clearly demonstrate that EX527 treatment leads to a significant reduction of the tumor burden *in vivo* in a xenograft NOKE6/E7-based mouse cancer model.

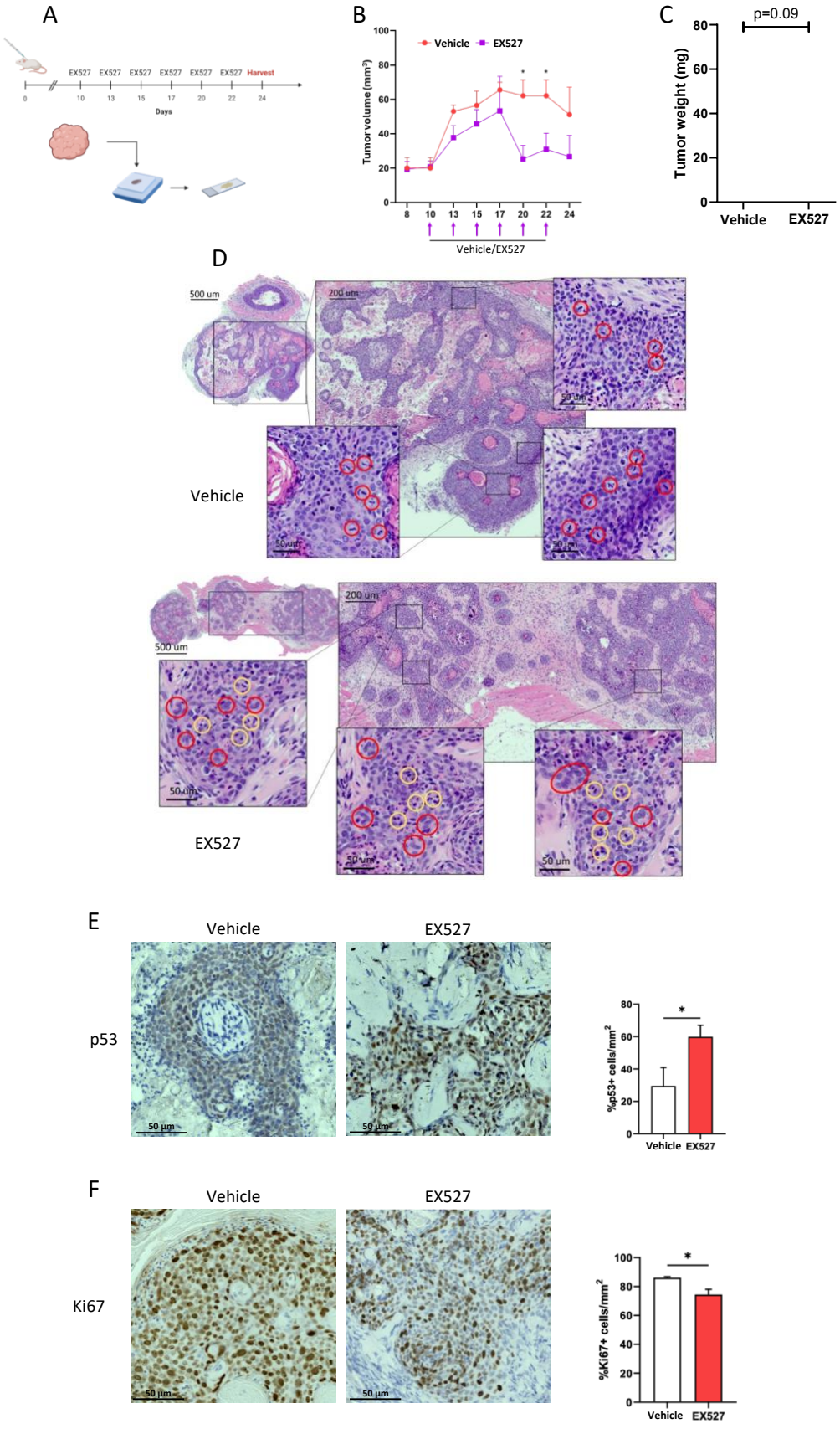

Figure 10. EX527 treatment reduces tumor burden in an allogeneic mouse model of HPV16-induced cancer. (A) Schematic illustration of the tumor model in which NOKE6/E7 cells were subcutaneously inoculated into the back of NSG mice. EX527 or vehicle treatments were administered intraperitoneally

every other day since day 10 after cell engraftment as depicted on the timeline. At day 24, mice were sacrificed, tumor collected and processed for paraffin embedding, and 5 µm-thickness section cutting for histologic analysis. **(B)** Tumor volume from mice treated as indicated in panel A was measured and plotted as mean volume of the tumors for each treatment. Error bars indicate SD. * $p < 0.05$, unpaired T-test. **(C)** Tumor weight from mice treated as indicated in panel A was determined at the end of the experiment. Each dot represents a data from a single mouse. Error bars indicate SD. **(D)** Representative images of H&E staining on tumors from mice treated with EX527 or vehicle. In tumors treated with vehicle (upper panel) red circles highlights atypic mitotic cells with misaligned chromosomes. In tumors treated with EX527 (lower panel) red and yellow circles indicate binucleated and apoptotic cells, respectively. **(E)** Representative images of p53 staining by immunohistochemistry on tumors from mice treated with EX527 or vehicle. Positive cells were quantified and plotted as percentage of positive cells per mm^2. Error bars indicate SD. * $p < 0.05$, unpaired T-test. **(F)** Representative images of Ki67 staining by immunohistochemistry on tumors treated with EX527 or vehicle. Positive cells were quantified and plotted as positive cells per mm^2. Error bars indicate SD. * $p < 0.05$, unpaired T-test.

5.3 Characterization of the SIRT1 molecular platform in HPV-transformed cells

To gain more insight into the mechanisms underlying SIRT1 action in the context of HPV-driven cancer, we have employed a proteomic approach to identify SIRT1 interacting partners in NOKE6/E7 cells in collaboration with Dr. Tiziana Bonaldi's group (Laboratory of Quantitative Proteomics and Gene Expression Regulation, IEO, Milan). This consisted in investigating the SIRT1 interactome under native conditions by mass-spectrometry (MS) analysis of SIRT1 co-immunoprecipitations (coIP) using the NOKE6/E7 cellular extracts as input. Label-free quantification from three coIP replicates revealed 793 proteins significantly co-enriched with SIRT1. The specificity of these interactions was confirmed by conducting coIPs in the presence of an excess of a soluble peptide competing with the bait for antibody binding, followed by assessing the selective removal of the bait and its interactors. Cross-referencing these two interatomic datasets has led to the identification of 182 high confidence interacting proteins (HCIPs) specifically associated with SIRT1. Gene ontology (GO) and STRING analysis of these 182 SIRT1 HCIPs showed that the preys localized in a panel of protein functions, including DNA repair, nuclear DNA replication, cell cycle, nucleocytoplasmic transport, cytoskeleton organization, Golgi vesicle transport, and viral gene expression (Figures 11A, 11B). Among these, we decided to focus our attention on the proteins of the network involved in DNA repair and nuclear DNA replication, including MCM7 and MCM4, belonging to the mini-chromosome maintenance (MCM) protein family. Remarkably, some members of this network, including

SMC3, RAD50, MCM7, and MCM4, had been previously reported as SIRT1 interactors (A. C. H. Chen et al., 2020; Y. Chen et al., 2012; Thakur et al., 2022; R.-H. Wang et al., 2014) (Figure 11C). For these reasons, we hypothesized the existence of a DNA-binding platform consisting of SIRT1 and the MCM complex at the replication origin to prevent excess replication and preserve genomic stability (Figure 11D). To verify this hypothesis, we performed a series of standard biochemical assays to validate the results obtained in the interactome analysis. Firstly, we immunoprecipitated SIRT1 in NOKE6/E7 and observed that when endogenous SIRT1 was pulled down, MCM7 and MCM4 were also detected (Figure 11E, left panel). At the same time, upon immunoprecipitation of endogenous MCM7 or MCM4 but not of control IgG, a low intensity band of SIRT1 was detected as well (Figure 11E, right panel). In addition, we performed a Proximity Ligation Assay (PLA) to confirm protein interactions (Figure 11F). As shown in figure 11F, we found that SIRT1 interacts with both MCM7 and MCM4 and we observed a higher percentage of PLA positive cells in NOKE6/E7 cells versus its HPV negative counterpart NOK cells (Figure 11F, left and middle panels). In addition, we performed a PLA for MCM7 and MCM4 confirming their interaction being part of the same complex and we found that this complex is expressed with a higher intensity in NOKE6/E7 cells versus NOK cells (Figure 11F, right panel).

Overall, these results confirm that SIRT1 interacts with MCM7 and MCM4 indicating the possible existence of the SIRT1-MCM complex platform.

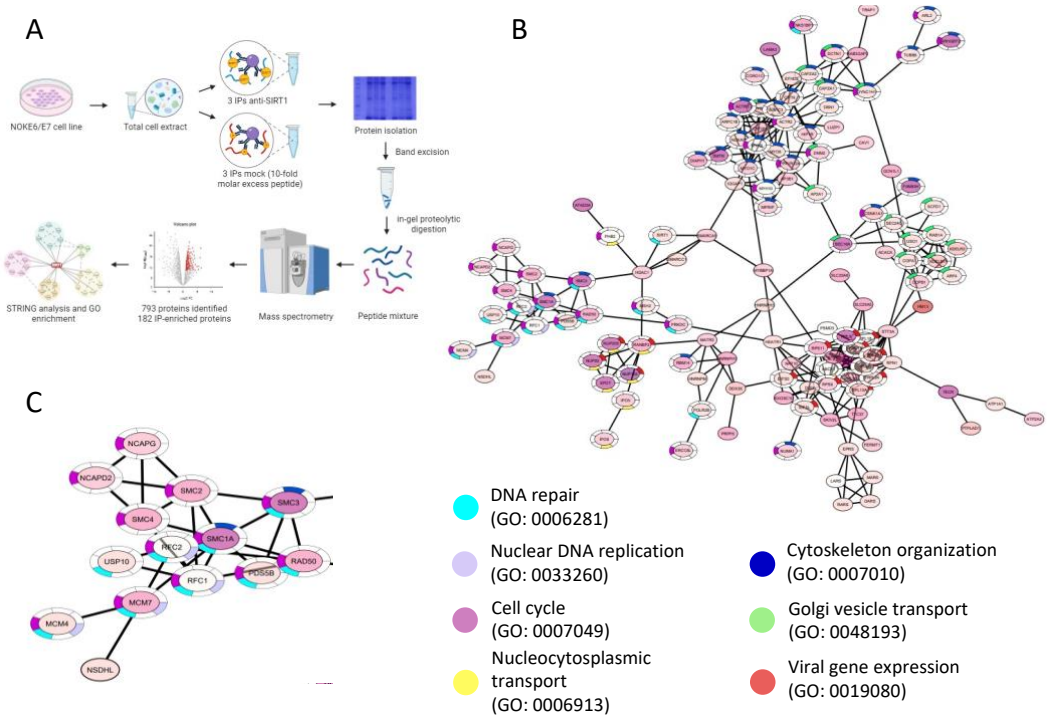
A
NOKE6/E7 cell line
Total cell extract
3 IPs anti-SIRT1
3 IPs mock (10-fold molar excess peptide)
Protein isolation
Band excision
In-gel proteolytic digestion
Peptide mixture
Mass spectrometry
793 proteins identified
182 IP-enriched proteins
STRING analysis and GO enrichment
B
C
NCAPG
NCAPD2
SMC2
SMC3
SMC4
SMC1A
RFC2
USP10
RAD50
RFC1
NBS1
MCM7
MCM4
NSDHL
DNA repair (GO: 0006281)
Nuclear DNA replication (GO: 0033260)
Cell cycle (GO: 0007049)
Nucleocytosplasmic transport (GO: 0006913)
Cytoskeleton organization (GO: 0007010)
Golgi vesicle transport (GO: 0048193)
Viral gene expression (GO: 0019080)

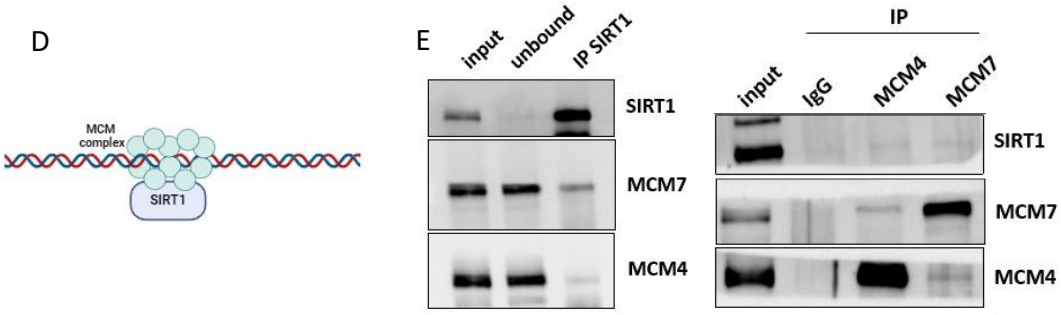
D
MCM complex
SIRT1
E
input
unbound
IP SIRT1
SIRT1
MCM7
MCM4
IP
input
IgG
MCM4
MCM7
SIRT1
MCM7
MCM4

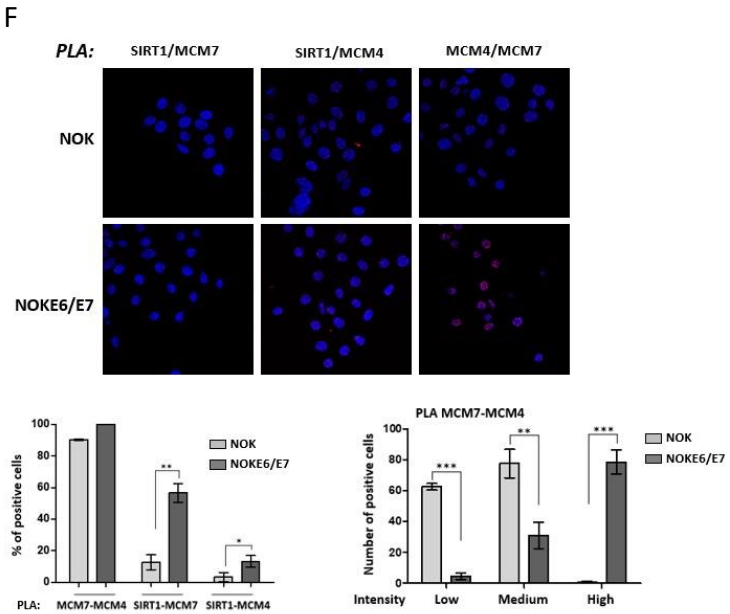
F
PLA:
SIRT1/MCM7
SIRT1/MCM4
MCM4/MCM7
NOK
NOKE6/E7
% of positive cells
NOK
NOKE6/E7
PLA:
MCM7-MCM4
SIRT1-MCM7
SIRT1-MCM4
PLA MCM7-MCM4
Number of positive cells
Intensity
Low
Medium
High

Figure 11. Characterization of the SIRT1 molecular platform in HPV-transformed cells. (A) Experimental workflow of a mass spectrometry analysis on NOKE6/E7 total cellular extract immunoprecipitated with anti-SIRT1 antibody. **(B)** Functional and physical interaction analysis of the SIRT1 interactome using the STRING interaction database. The STRING networks were visualized using Cytoscape and a gene ontology (GO) analysis was performed. **(C)** Highlight of the STRING network involved in DNA repair, DNA replication, and cell cycle. **(D)** Schematic illustration of the SIRT1-MCM4-MCM7 molecular platform bound to the DNA replication origin. **(E)** Total cell extracts from NOKE6/E7 cells were immunoprecipitated using anti-SIRT1, anti-MCM7, anti-MCM4, and anti-IgG antibodies as control and immunoblotted with the indicated antibodies. The image displayed is representative of 3 biological replicates. **(F)** Representative images of proximity ligation assay performed between SIRT1 and MCM7 (left panels), SIRT1 and MCM4 (middle panels), and MCM7 and MCM4 (right panels) on NOK and NOKE6/E7 cells. The percentage of PLA positive cells and PLA signal intensity was quantitated using QuPath software. Errors bars indicate SD. * $p < 0.05$, **$p<0.01$, *** $p < 0.001$, unpaired T-test.

6. DISCUSSION

Papillomaviruses are small, non-enveloped, epitheliotropic, double-stranded DNA virus that infect cutaneous and mucosal epithelia in a wide variety of vertebrates in a species-specific manner inducing cellular proliferation. Human papillomaviruses (HPVs) are organized into five genera (*alpha, beta, gamma, mu,* and *nu*) and are divided into either "cutaneous" or "mucosal". Based on their transforming ability, mucosal HPVs are also classified as "high-risk" and "low-risk" (Doorbar et al., 2015; Egawa et al., 2015; Nelson & Mirabello, 2023). High-risk HPVs (hrHPVs), among which HPV16 and HPV18 are the most frequent, are associated with cervical and other anogenital cancers and with head and neck cancers, primarily OPSCCs. While virtually all cervical cancers are HPV-driven, the fraction of OPSCCs likely arising from HPV infection has been estimated to be around 20% and is associated with a more favourable prognosis than that of HPV-negative OPSCC (Caudell et al., 2022; Ghiani & Chiocca, 2022; Lechner et al., 2022). The treatment for these HPV-associated cancers currently involves radiotherapy, chemotherapy, or surgery, all with devastating effects on the targeted anatomical sites, so there is an urgent clinical need for alternative approaches that may allow de-escalating current drug therapies to improve patient outcomes while reducing treatment-related acute and long-term toxicities.

In this context, SIRT1 is the principal NAD+ dependent deacetylase in mammalian cells involved in a broad range of biological activities. In particular, SIRT1 catalyses the deacetylation of its substrates, which include histone and non-histone proteins, such as p53 (Roth & Chen, 2014). SIRT1-dependent p53 deacetylation on Lys382 residue decreases p53-mediated transcriptional activity, inhibiting cell cycle arrest and promoting cell survival and proliferation (T. F. Liu & McCall, 2013; Luo et al., 2001; Roth & Chen, 2014). In addition, SIRT1 has already been reported to be strongly upregulated in HPV-positive cells and cervical intraepithelial neoplasia (CIN) in an E7-dependent fashion (Velez-Perez et al., 2017). For these reasons, the group I joined for my internship has recently demonstrated the role of SIRT1 in HPV-associated cancers. Specifically, they demonstrated that SIRT1 pharmacological inhibition, using EX527, restores a functional K382-acetylated p53 leading to cell cycle arrest at G0/G1 phase and reduction of cell survival and clonogenicity compared to HPV-negative cells, and in particular in NOKE6/E7 cells (Lo Cigno et al., 2023). According to these results, we decided to use more physiological systems to better understand the role of SIRT1 in HPV-induced carcinogenesis and confirm the antiproliferative effect of EX527 observed *in vitro*. In this regard, we generated a three-dimensional system that recapitulates the structure of the stratified squamous

epithelia, namely NOKE6/E7 organotypic raft cultures, and we observed that EX527 treatment leads to a reduced NOKE6/E7 cell proliferation and invasion capability, as confirmed by the significant reduction of the proliferation marker MCM7 and a lower EdU incorporation (Figures 9C, 9D). In HPV-driven oncogenesis, MCM7 is commonly used as a potential proliferation marker since its upregulation has been steadily observed in both *in vitro* and *in vivo* setting, including human cancers, and it is considered an informative biomarker of E6/E7 deregulation. Remarkably, similar results were observed in a NOKE6/E7-based allogeneic HPV16-induced mouse cancer model. In particular, we observed a significant reduction in tumor volume and weight, p53 restoration, and a reduction of the proliferation marker Ki67 in mice treated with EX527 when compared to vehicle-treated mice (Figures 10). These findings confirm the antiproliferative effect of the SIRT1 inhibitor supporting the hypothesis that SIRT1 upregulation is a key mechanism of HPV-driven oncogenesis and that it could be considered as important therapeutic target. Hence, to gain more insight into the molecular mechanism underlying SIRT1 action in the context of HPV-driven cancer, we evaluated the SIRT1 interactome in NOKE6/E7 cells through a mass spectrometry analysis in collaboration with Dr. Bonaldi's group. We identified a panel of interacting proteins involved in a variety of cellular processes, such as DNA repair and DNA replication, including MCM7 and MCM4, belonging to the mini-chromosome maintenance (MCM) protein family, SMC3, and Rad50 (Figures 11B, 11C). Given that these interactions have already been reported in the literature (A. C. H. Chen et al., 2020; Y. Chen et al., 2012; Thakur et al., 2022; R.-H. Wang et al., 2014), we decided to focus our attention on this STRING network and we started to validate SIRT1 interaction with MCM7 and MCM4 using a co-immunoprecipitation assay and a Proximity Ligation Assay (PLA) in NOKE6/E7 cells. In addition, we observed that the percentage of PLA-positive cells in NOKE6/E7 cells was higher compared to that observed in its counterpart HPV-negative NOK cells (Figure 11E, 11F). Based on these findings and considering that MCM7 is a replication factor that binds to DNA double strand at replication origins in the late G1 phase, forms the pre-RC complex during cell cycle progression, and alleviates endogenous DNA replication stress, we hypothesized the existence of a chromatin-binding platform consisting of SIRT1 and the MCM complex at the replication origin to prevent excess replication and preserve genomic stability (Figure 11D). Therefore, further studies are necessary to better characterize this platform and to evaluate how the interaction among these proteins is modulated.

7. BIBLIOGRAFY

Abid Ali, F., Renault, L., Gannon, J., Gahlon, H. L., Kotecha, A., Zhou, J. C., Rueda, D., & Costa, A. (2016). Cryo-EM structures of the eukaryotic replicative helicase bound to a translocation substrate. *Nature Communications*, *7*, 10708. https://doi.org/10.1038/ncomms10708

Allison, S. J., Jiang, M., & Milner, J. (2009). Oncogenic viral protein HPV E7 up-regulates the SIRT1 longevity protein in human cervical cancer cells. *Aging*, *1*(3), 316–327. https://doi.org/10.18632/aging.100028

Ang, K. K., Harris, J., Wheeler, R., Weber, R., Rosenthal, D. I., Nguyen-Tân, P. F., Westra, W. H., Chung, C. H., Jordan, R. C., Lu, C., Kim, H., Axelrod, R., Silverman, C. C., Redmond, K. P., & Gillison, M. L. (2010). Human papillomavirus and survival of patients with oropharyngeal cancer. *The New England Journal of Medicine*, *363*(1), 24–35. https://doi.org/10.1056/NEJMoa0912217

Asaka, R., Miyamoto, T., Yamada, Y., Ando, H., Mvunta, D. H., Kobara, H., & Shiozawa, T. (2015). Sirtuin 1 promotes the growth and cisplatin resistance of endometrial carcinoma cells: A novel therapeutic target. *Laboratory Investigation*, *95*(12), 1363–1373. https://doi.org/10.1038/labinvest.2015.119

Balsitis, S., Dick, F., Dyson, N., & Lambert, P. F. (2006). Critical Roles for Non-pRb Targets of Human Papillomavirus Type 16 E7 in Cervical Carcinogenesis. *Cancer research*, *66*(19), 9393–9400. https://doi.org/10.1158/0008-5472.CAN-06-0984

Bergvall, M., Melendy, T., & Archambault, J. (2013). The E1 proteins. *Virology*, *445*(1), 35–56. https://doi.org/10.1016/j.virol.2013.07.020

Bochman, M. L., & Schwacha, A. (2009). The Mcm Complex: Unwinding the Mechanism of a Replicative Helicase. *Microbiology and Molecular Biology Reviews*, *73*(4), 652–683. https://doi.org/10.1128/mmbr.00019-09

Brake, T., Connor, J. P., Petereit, D. G., & Lambert, P. F. (2003). Comparative Analysis of Cervical Cancer in Women and in a Human Papillomavirus-Transgenic Mouse Model: Identification of Minichromosome Maintenance Protein 7 as an Informative Biomarker for Human Cervical Cancer. *Cancer Research*, *63*(23), 8173–8180.

Buck, C. B., Day, P. M., & Trus, B. L. (2013). The papillomavirus major capsid protein L1. *Virology*, *445*(1), 169–174. https://doi.org/10.1016/j.virol.2013.05.038

Burd, E. M. (2003). Human Papillomavirus and Cervical Cancer. *Clinical Microbiology Reviews*, *16*(1), 1–17. https://doi.org/10.1128/cmr.16.1.1-17.2003

Burk, R. D., Harari, A., & Chen, Z. (2013). Human papillomavirus genome variants. *Virology*, *445*(1), 232–243. https://doi.org/10.1016/j.virol.2013.07.018

Caudell, J. J., Gillison, M. L., Maghami, E., Spencer, S., Pfister, D. G., Adkins, D., Birkeland, A. C., Brizel, D. M., Busse, P. M., Cmelak, A. J., Colevas, A. D., Eisele, D. W., Galloway, T., Geiger, J. L., Haddad, R. I., Hicks, W. L., Hitchcock, Y. J., Jimeno, A., Leizman, D., … Darlow, S. D. (2022). NCCN Guidelines® Insights: Head and Neck Cancers, Version 1.2022. *Journal of the National Comprehensive Cancer Network: JNCCN*, *20*(3), 224–234. https://doi.org/10.6004/jnccn.2022.0016

Chen, A. C. H., Peng, Q., Fong, S. W., Yeung, W. S. B., & Lee, Y. L. (2020). Sirt1 is regulated by miR-135a and involved in DNA damage repair during mouse cellular reprogramming. *Aging (Albany NY)*, *12*(8), 7431–7447. https://doi.org/10.18632/aging.103090

Chen, H., Lin, R., Zhang, Z., Wei, Q., Zhong, Z., Huang, J., & Xu, Y. (2019). Sirtuin 1 knockdown inhibits glioma cell proliferation and potentiates temozolomide toxicity via facilitation of reactive oxygen species generation. *Oncology Letters*, *17*(6), 5343–5350. https://doi.org/10.3892/ol.2019.10235

Chen, Y., Zhao, W., Yang, J. S., Cheng, Z., Luo, H., Lu, Z., Tan, M., Gu, W., & Zhao, Y. (2012). Quantitative Acetylome Analysis Reveals the Roles of SIRT1 in Regulating Diverse Substrates and Cellular Pathways*. *Molecular & Cellular Proteomics*, *11*(10), 1048–1062. https://doi.org/10.1074/mcp.M112.019547

Das, D., Smith, N., Wang, X., & Morgan, I. M. (2017). The Deacetylase SIRT1 Regulates the Replication Properties of Human Papillomavirus 16 E1 and E2. *Journal of Virology*, *91*(10), e00102-17. https://doi.org/10.1128/JVI.00102-17

Das, M., Prasad, S. B., Yadav, S. S., Govardhan, H. B., Pandey, L. K., Singh, S., Pradhan, S., & Narayan, G. (2013). Over Expression of Minichromosome Maintenance Genes is Clinically Correlated to Cervical Carcinogenesis. *PLOS ONE*, *8*(7), e69607. https://doi.org/10.1371/journal.pone.0069607

de Freitas, A. C., de Oliveira, T. H. A., Barros, M. R., & Venuti, A. (2017). hrHPV E5 oncoprotein: Immune evasion and related immunotherapies. *Journal of Experimental & Clinical Cancer Research*, *36*(1), 71. https://doi.org/10.1186/s13046-017-0541-1

Dewar, J. M., Low, E., Mann, M., Räschle, M., & Walter, J. C. (2017). CRL2Lrr1 promotes unloading of the vertebrate replisome from chromatin during replication termination. *Genes & Development*, *31*(3), 275–290. https://doi.org/10.1101/gad.291799.116

Doorbar, J. (2013). The E4 protein; structure, function and patterns of expression. *Virology*, *445*(1), 80–98. https://doi.org/10.1016/j.virol.2013.07.008

Doorbar, J., Egawa, N., Griffin, H., Kranjec, C., & Murakami, I. (2015). Human papillomavirus molecular biology and disease association. *Reviews in Medical Virology*, *25*(S1), 2–23. https://doi.org/10.1002/rmv.1822

Doorbar, J., Quint, W., Banks, L., Bravo, I. G., Stoler, M., Broker, T. R., & Stanley, M. A. (2012). The Biology and Life-Cycle of Human Papillomaviruses. *Vaccine*, *30*, F55–F70. https://doi.org/10.1016/j.vaccine.2012.06.083

Douglas, M. E., Ali, F. A., Costa, A., & Diffley, J. F. X. (2018). The mechanism of eukaryotic CMG helicase activation. *Nature*, *555*(7695), 265–268. https://doi.org/10.1038/nature25787

Drissi, R., Chauvin, A., McKenna, A., Lévesque, D., Blais-Brochu, S., Jean, D., & Boisvert, F.-M. (2018). Destabilization of the MiniChromosome Maintenance (MCM) complex modulates the cellular response to DNA double strand breaks. *Cell Cycle*, *17*(23), 2593–2609. https://doi.org/10.1080/15384101.2018.1553336

Egawa, N., & Doorbar, J. (2017). The low-risk papillomaviruses. *Virus Research*, *231*, 119–127. https://doi.org/10.1016/j.virusres.2016.12.017

Egawa, N., Egawa, K., Griffin, H., & Doorbar, J. (2015). Human Papillomaviruses; Epithelial Tropisms, and the Development of Neoplasia. *Viruses*, *7*(7), Articolo 7. https://doi.org/10.3390/v7072802

Estêvão, D., Costa, N. R., Gil da Costa, R. M., & Medeiros, R. (2019). Hallmarks of HPV carcinogenesis: The role of E6, E7 and E5 oncoproteins in cellular malignancy. *Biochimica et Biophysica Acta (BBA) - Gene Regulatory Mechanisms*, *1862*(2), 153–162. https://doi.org/10.1016/j.bbagrm.2019.01.001

Gheit, T. (2019). Mucosal and Cutaneous Human Papillomavirus Infections and Cancer Biology. *Frontiers in Oncology*, *9*, 355. https://doi.org/10.3389/fonc.2019.00355

Ghiani, L., & Chiocca, S. (2022). High Risk-Human Papillomavirus in HNSCC: Present and Future Challenges for Epigenetic Therapies. *International Journal of Molecular Sciences*, *23*(7), Articolo 7. https://doi.org/10.3390/ijms23073483

Graham, S. V. (2017). The human papillomavirus replication cycle, and its links to cancer progression: A comprehensive review. *Clinical Science*, *131*(17), 2201–2221. https://doi.org/10.1042/CS20160786

Harden, M. E., & Munger, K. (2017). Human papillomavirus molecular biology. *Mutation Research/Reviews in Mutation Research*, *772*, 3–12. https://doi.org/10.1016/j.mrrev.2016.07.002

Honeycutt, K. A., Chen, Z., Koster, M. I., Miers, M., Nuchtern, J., Hicks, J., Roop, D. R., & Shohet, J. M. (2006). Deregulated minichromosomal maintenance protein MCM7 contributes to oncogene driven tumorigenesis. *Oncogene*, *25*(29), 4027–4032. https://doi.org/10.1038/sj.onc.1209435

Hong, S., & Laimins, L. A. (2013). Regulation of the life cycle of HPVs by differentiation and the DNA damage response. *Future microbiology*, *8*, 1547–1557. https://doi.org/10.2217/fmb.13.127

Huffman, D. M., Grizzle, W. E., Bamman, M. M., Kim, J., Eltoum, I. A., Elgavish, A., & Nagy, T. R. (2007). SIRT1 Is Significantly Elevated in Mouse and Human Prostate Cancer. *Cancer Research*, *67*(14), 6612–6618. https://doi.org/10.1158/0008-5472.CAN-07-0085

Jiang, W., Jiang, P., Yang, R., & Liu, D.-F. (2018). Functional role of SIRT1-induced HMGB1 expression and

acetylation in migration, invasion and angiogenesis of ovarian cancer. *European Review for Medical and Pharmacological Sciences*, *22*(14), 4431–4439. https://doi.org/10.26355/eurrev_201807_15494

Johnson, D. E., Burtness, B., Leemans, C. R., Lui, V. W. Y., Bauman, J. E., & Grandis, J. R. (2020). Head and neck squamous cell carcinoma. *Nature reviews. Disease primers*, *6*(1), 92. https://doi.org/10.1038/s41572-020-00224-3

Kang, S. D., Chatterjee, S., Alam, S., Salzberg, A. C., Milici, J., van der Burg, S. H., & Meyers, C. (2018). Effect of Productive Human Papillomavirus 16 Infection on Global Gene Expression in Cervical Epithelium. *Journal of Virology*, *92*(20), 10.1128/jvi.01261-18. https://doi.org/10.1128/jvi.01261-18

Kines, R. C., & Schiller, J. T. (2022). Harnessing Human Papillomavirus' Natural Tropism to Target Tumors. *Viruses*, *14*(8), 1656. https://doi.org/10.3390/v14081656

Kühne, C., & Banks, L. (1998). E3-Ubiquitin Ligase/E6-AP Links Multicopy Maintenance Protein 7 to the Ubiquitination Pathway by a Novel Motif, the L2G Box*. *Journal of Biological Chemistry*, *273*(51), 34302–34309. https://doi.org/10.1074/jbc.273.51.34302

Kukimoto, I., Aihara, S., Yoshiike, K., & Kanda, T. (1998). Human Papillomavirus Oncoprotein E6 Binds to the C-Terminal Region of Human Minichromosome Maintenance 7 Protein. *Biochemical and Biophysical Research Communications*, *249*(1), 258–262. https://doi.org/10.1006/bbrc.1998.9066

Langsfeld, E. S., Bodily, J. M., & Laimins, L. A. (2015). The Deacetylase Sirtuin 1 Regulates Human Papillomavirus Replication by Modulating Histone Acetylation and Recruitment of DNA Damage Factors NBS1 and Rad51 to Viral Genomes. *PLOS Pathogens*, *11*(9), e1005181. https://doi.org/10.1371/journal.ppat.1005181

Lechner, M., Liu, J., Masterson, L., & Fenton, T. R. (2022). HPV-associated oropharyngeal cancer: Epidemiology, molecular biology and clinical management. *Nature Reviews Clinical Oncology*, *19*(5), 306–327. https://doi.org/10.1038/s41571-022-00603-7

Li, X., Jiang, Z., Li, X., & Zhang, X. (2018). SIRT1 overexpression protects non-small cell lung cancer cells against osteopontin-induced epithelial-mesenchymal transition by suppressing NF-κB signaling. *OncoTargets and Therapy*, *11*, 1157–1171. https://doi.org/10.2147/OTT.S137146

Li, Z., Chen, L., Kabra, N., Wang, C., Fang, J., & Chen, J. (2009). Inhibition of SUV39H1 Methyltransferase Activity by DBC1*. *Journal of Biological Chemistry*, *284*(16), 10361–10366. https://doi.org/10.1074/jbc.M900956200

Lin, Z., & Fang, D. (2013). The Roles of SIRT1 in Cancer. *Genes & Cancer*, *4*(3–4), 97–104. https://doi.org/10.1177/1947601912475079

Liu, L., Liu, C., Zhang, Q., Shen, J., Zhang, H., Shan, J., Duan, G., Guo, D., Chen, X., Cheng, J., Xu, Y., Yang, Z., Yao, C., Lai, M., & Qian, C. (2016). SIRT1-mediated transcriptional regulation of SOX2 is important for self-renewal of liver cancer stem cells. *Hepatology*, *64*(3), 814. https://doi.org/10.1002/hep.28690

Liu, T. F., & McCall, C. E. (2013). Deacetylation by SIRT1 Reprograms Inflammation and Cancer. *Genes & Cancer*, *4*(3–4), 135–147. https://doi.org/10.1177/1947601913476948

Lo Cigno, I., Calati, F., Girone, C., Borgogna, C., Venuti, A., Boldorini, R., & Gariglio, M. (2023). SIRT1 is an actionable target to restore p53 function in HPV-associated cancer therapy. *British Journal of Cancer*, *129*(11), 1863–1874. https://doi.org/10.1038/s41416-023-02465-x

Luo, J., Nikolaev, A. Y., Imai, S., Chen, D., Su, F., Shiloh, A., Guarente, L., & Gu, W. (2001). Negative Control of p53 by Sir2α Promotes Cell Survival under Stress. *Cell*, *107*(2), 137–148. https://doi.org/10.1016/S0092-8674(01)00524-4

Masai, H., Matsumoto, S., You, Z., Yoshizawa-Sugata, N., & Oda, M. (2010, giugno 9). *Eukaryotic Chromosome DNA Replication: Where, When, and How?* (world) [Review-article]. Https://Doi.Org/10.1146/Annurev.Biochem.052308.103205; Annual Reviews. https://doi.org/10.1146/annurev.biochem.052308.103205

McBride, A. A. (2013). The Papillomavirus E2 proteins. *Virology*, *445*(1), 57–79. https://doi.org/10.1016/j.virol.2013.06.006

McBride, A. A. (2022). Human papillomaviruses: Diversity, infection and host interactions. *Nature Reviews Microbiology*, *20*(2), Articolo 2. https://doi.org/10.1038/s41579-021-00617-5

McBride, A. A., & Warburton, A. (2017). The role of integration in oncogenic progression of HPV-associated cancers. *PLOS Pathogens*, *13*(4), e1006211. https://doi.org/10.1371/journal.ppat.1006211

Meagher, M., Epling, L. B., & Enemark, E. J. (2019). DNA translocation mechanism of the MCM complex and implications for replication initiation. *Nature Communications*, *10*(1), Articolo 1. https://doi.org/10.1038/s41467-019-11074-3

Moody, C. A. (2022). Regulation of the Innate Immune Response during the Human Papillomavirus Life Cycle. *Viruses*, *14*(8), 1797. https://doi.org/10.3390/v14081797

Nelson, C. W., & Mirabello, L. (2023). Human papillomavirus genomics: Understanding carcinogenicity. *Tumour Virus Research*, *15*, 200258. https://doi.org/10.1016/j.tvr.2023.200258

Neves, H., & Kwok, H. F. (2017). In sickness and in health: The many roles of the minichromosome maintenance proteins. *Biochimica Et Biophysica Acta. Reviews on Cancer*, *1868*(1), 295–308. https://doi.org/10.1016/j.bbcan.2017.06.001

Powell, S. F., Vu, L., Spanos, W. C., & Pyeon, D. (2021). The Key Differences between Human Papillomavirus-Positive and -Negative Head and Neck Cancers: Biological and Clinical Implications. *Cancers*, *13*(20), Articolo 20. https://doi.org/10.3390/cancers13205206

Radiation Therapy Oncology Group. (2023). *A Phase III Trial of Concurrent Radiation and Chemotherapy for Advanced Head and Neck Carcinomas* (Clinical trial registration NCT00047008). clinicaltrials.gov. https://clinicaltrials.gov/study/NCT00047008

Ren, N. S. X., Ji, M., Tokar, E. J., Busch, E. L., Xu, X., Lewis, D., Li, X., Jin, A., Zhang, Y., Wu, W. K. K., Huang, W., Li, L., Fargo, D. C., Keku, T. O., Sandler, R. S., & Li, X. (2017). Haploinsufficiency of SIRT1 Enhances Glutamine Metabolism and Promotes Cancer Development. *Current Biology*, *27*(4), 483–494. https://doi.org/10.1016/j.cub.2016.12.047

Roth, M., & Chen, W. Y. (2014). Sorting out functions of sirtuins in cancer. *Oncogene*, *33*(13), 1609–1620. https://doi.org/10.1038/onc.2013.120

Sabatini, M. E., & Chiocca, S. (2020). Human papillomavirus as a driver of head and neck cancers. *British Journal of Cancer*, *122*(3), 306–314. https://doi.org/10.1038/s41416-019-0602-7

Scarth, J. A., Patterson, M. R., Morgan, E. L., & Macdonald, A. (2021). The human papillomavirus oncoproteins: A review of the host pathways targeted on the road to transformation. *Journal of General Virology*, *102*(3), 001540. https://doi.org/10.1099/jgv.0.001540

Shanmugasundaram, S., & You, J. (2017). Targeting Persistent Human Papillomavirus Infection. *Viruses*, *9*(8), Articolo 8. https://doi.org/10.3390/v9080229

So, D., Shin, H.-W., Kim, J., Lee, M., Myeong, J., Chun, Y.-S., & Park, J.-W. (2018). Cervical cancer is addicted to SIRT1 disarming the AIM2 antiviral defense. *Oncogene*, *37*(38), 5191–5204. https://doi.org/10.1038/s41388-018-0339-4

Sun, Y., Wang, Z., Qiu, S., & Wang, R. (2021). Therapeutic strategies of different HPV status in Head and Neck Squamous Cell Carcinoma. *International Journal of Biological Sciences*, *17*(4), 1104–1118. https://doi.org/10.7150/ijbs.58077

Thakur, B. L., Baris, A. M., Fu, H., Redon, C. E., Pongor, L. S., Mosavarpour, S., Gross, J. M., Jang, S.-M., Sebastian, R., Utani, K., Jenkins, L. M., Indig, F. E., & Aladjem, M. I. (2022). Convergence of SIRT1 and ATR signaling to modulate replication origin dormancy. *Nucleic Acids Research*, *50*(9), 5111–5128. https://doi.org/10.1093/nar/gkac299

Toyokawa, G., Masuda, K., Daigo, Y., Cho, H.-S., Yoshimatsu, M., Takawa, M., Hayami, S., Maejima, K., Chino, M., Field, H. I., Neal, D. E., Tsuchiya, E., Ponder, B. A. J., Maehara, Y., Nakamura, Y., & Hamamoto, R. (2011). Minichromosome Maintenance Protein 7 is a potential therapeutic target in human cancer and a novel prognostic marker of non-small cell lung cancer. *Molecular Cancer*, *10*. Scopus. https://doi.org/10.1186/1476-4598-10-65

Vaquero, A., Scher, M., Erdjument-Bromage, H., Tempst, P., Serrano, L., & Reinberg, D. (2007). SIRT1 regulates the histone methyl-transferase SUV39H1 during heterochromatin formation. *Nature*, *450*(7168), 440–444. https://doi.org/10.1038/nature06268

Vaquero, A., Scher, M., Lee, D., Erdjument-Bromage, H., Tempst, P., & Reinberg, D. (2004). Human SirT1 Interacts with Histone H1 and Promotes Formation of Facultative Heterochromatin. *Molecular Cell*, *16*(1), 93–105. https://doi.org/10.1016/j.molcel.2004.08.031

Vaziri, H., Dessain, S. K., Eaton, E. N., Imai, S.-I., Frye, R. A., Pandita, T. K., Guarente, L., & Weinberg, R. A. (2001). hSIR2SIRT1 functions as an NAD-dependent p53 deacetylase. *Cell*, *107*(2), 149–159. Scopus. https://doi.org/10.1016/S0092-8674(01)00527-X

Velez-Perez, A., Wang, X. I., Li, M., & Zhang, S. (2017). SIRT1 overexpression in cervical squamous intraepithelial lesions and invasive squamous cell carcinoma. *Human Pathology*, *59*, 102–107. https://doi.org/10.1016/j.humpath.2016.09.019

Wang, F., Li, Z., Zhou, J., Wang, G., Zhang, W., Xu, J., & Liang, A. (2021). SIRT1 regulates the phosphorylation and degradation of P27 by deacetylating CDK2 to promote T-cell acute lymphoblastic leukemia progression. *Journal of Experimental & Clinical Cancer Research*, *40*(1), 259. https://doi.org/10.1186/s13046-021-02071-w

Wang, J. W., & Roden, R. B. S. (2013). L2, the minor capsid protein of papillomavirus. *Virology*, *445*(1), 175–186. https://doi.org/10.1016/j.virol.2013.04.017

Wang, R.-H., Lahusen, T. J., Chen, Q., Xu, X., Jenkins, L. M. M., Leo, E., Fu, H., Aladjem, M., Pommier, Y., Appella, E., & Deng, C.-X. (2014). SIRT1 Deacetylates TopBP1 and Modulates Intra-S-Phase Checkpoint and DNA Replication Origin Firing. *International Journal of Biological Sciences*, *10*(10), 1193–1202. https://doi.org/10.7150/ijbs.11066

Wang, Y., Chen, H., Zhang, J., Cheng, A. S. L., Yu, J., To, K. F., & Kang, W. (2020). MCM family in gastrointestinal cancer and other malignancies: From functional characterization to clinical implication. *Biochimica et Biophysica Acta (BBA) - Reviews on Cancer*, *1874*(2), 188415. https://doi.org/10.1016/j.bbcan.2020.188415

Wilson, R., & Laimins, L. A. (2005). Differentiation of HPV-containing cells using organotypic «raft» culture or methylcellulose. *Methods in Molecular Medicine*, *119*, 157–169. https://doi.org/10.1385/1-59259-982-6:157

Wu, Q.-J., Zhang, T.-N., Chen, H.-H., Yu, X.-F., Lv, J.-L., Liu, Y.-Y., Liu, Y.-S., Zheng, G., Zhao, J.-Q., Wei, Y.-F., Guo, J.-Y., Liu, F.-H., Chang, Q., Zhang, Y.-X., Liu, C.-G., & Zhao, Y.-H. (2022). The sirtuin family in health and disease. *Signal Transduction and Targeted Therapy*, *7*(1), 1–74. https://doi.org/10.1038/s41392-022-01257-8

Xia, Y., Sonneville, R., Jenkyn-Bedford, M., Ji, L., Alabert, C., Hong, Y., Yeeles, J. T. P., & Labib, K. P. M. (2023). DNSN-1 recruits GINS for CMG helicase assembly during DNA replication initiation in C. elegans. *Science (New York, N.Y.)*, *381*(6664), eadi4932. https://doi.org/10.1126/science.adi4932

Xu, J., You, C., Zhang, S., Huang, S., Cai, B., Wu, Z., & Li, H. (2006). Angiogenesis and cell proliferation in human craniopharyngioma xenografts in nude mice. *Journal of Neurosurgery: Pediatrics*, *105*(4), 306–310. https://doi.org/10.3171/ped.2006.105.4.306

Xu, Y., Qin, Q., Chen, R., Wei, C., & Mo, Q. (2018). SIRT1 promotes proliferation, migration, and invasion of breast cancer cell line MCF-7 by upregulating DNA polymerase delta1 (POLD1). *Biochemical and Biophysical Research Communications*, *502*(3), 351–357. https://doi.org/10.1016/j.bbrc.2018.05.164

Yang, R., Klimentová, J., Göckel-Krzikalla, E., Ly, R., Gmelin, N., Hotz-Wagenblatt, A., Řehulková, H., Stulík, J., Rösl, F., & Niebler, M. (2019). Combined Transcriptome and Proteome Analysis of Immortalized Human Keratinocytes Expressing Human Papillomavirus 16 (HPV16) Oncogenes Reveals Novel Key Factors and Networks in HPV-Induced Carcinogenesis. *mSphere*, *4*(2), 10.1128/msphere.00129-19. https://doi.org/10.1128/msphere.00129-19

Ying, C. Y., & Gautier, J. (2005). The ATPase activity of MCM2-7 is dispensable for pre-RC assembly but is

required for DNA unwinding. *EMBO Journal*, *24*(24), 4334–4344. Scopus. https://doi.org/10.1038/sj.emboj.7600892

You, E. L., Henry, M., & Zeitouni, A. G. (2019). Human papillomavirus–associated oropharyngeal cancer: Review of current evidence and management. *Current Oncology*, *26*(2), 119–123. https://doi.org/10.3747/co.26.4819

Yu, L., Majerciak, V., & Zheng, Z.-M. (2022). HPV16 and HPV18 Genome Structure, Expression, and Post-Transcriptional Regulation. *International Journal of Molecular Sciences*, *23*(9), Articolo 9. https://doi.org/10.3390/ijms23094943

Zhou, C., Tuong, Z. K., & Frazer, I. H. (2019). Papillomavirus Immune Evasion Strategies Target the Infected Cell and the Local Immune System. *Frontiers in Oncology*, *9*. https://www.frontiersin.org/articles/10.3389/fonc.2019.00682

zur Hausen, H. (1996). Viruses in human tumors—Reminiscences and perspectives. *Advances in Cancer Research*, *68*, 1–22.